PhD degree in Systems Medicine

(curriculum in Molecular Oncology)

European School of Molecular Medicine (SEMM),

University of Milan and University of Naples "Federico II"

Settore disciplinare: MED/04

Lack of p21 expression in tumor-associated APCs

triggers the activation

of a potent anti-tumor immune response

Olga Tanaskovic

IEO, Milan

Matricola n. R11138

Supervisor: Professor Pier Giuseppe Pelicci,

European Institute of Oncology (IEO), Milan

Added Supervisor: Dr. Maria Vittoria Verga Falzacappa,

European Institute of Oncology (IEO), Milan

Anno accademico 2017-2018

TABLE OF CONTENTS

1. LIST OF ABBREVIATIONS

AML = Acute myeloid leukaemia

APC = Antigen-presenting cell

APL = Acute promyelocytic leukaemia

BM = Bone marrow

BMDM = Bone marrow-derived macrophage

CD = Cluster of differentiation

CDK = Cyclin-dependent kinase

CDKi = Cyclin-dependent kinase inhibitor

CIP/Kip = CDK interacting protein/Kinase inhibitory protein

CSC = Cancer stem cell

CTLA-4 = Cytotoxic T-lymphocyte associated protein 4

CX3CR1 = CX3 Chemokine receptor 1

DC = Dendritic cell

ECM = Extracellular matrix

ENU = N-ethyl-N-nitrosourea

ErbB2 = Receptor tyrosin-protein kinase erbB2

GVHD = Graft versus host disease

HSC = Hematopoietic stem cell

HSPCs = Hematopoietic stem and progenitor cells

IC = Immune complex

IFN = Interferon

IL = Interleukin

LPS = Lipopolysaccharide

LSC = Leukaemia stem cell

Lin = Lineage

MDSC = Myeloid-derived suppressor cell

MHC = Major histocompatibility complex

MNC = Mononuclear cell

NK = Natural killer cell

NPM = Nucleophosmin

NSCLC = Non-small cell lung cancer

PCNA = Proliferating cell nuclear antigen

RBC = Red blood cell

ROS = Reactive oxygen species

SC = Stem cell

SLE = Systemic lupus erythematosus

T-ALL = T-cell acute lymphoblastic leukaemia

T-reg = Regulatory T cell

TAM = Tumor-associated macrophage

TCR = T cell receptor

TGF-β = Transforming growth factor beta

TIL = Tumor-infiltrating lymphocyte

TLR = Toll-like receptor

TME = Tumor microenvironment

TNF = Tumor necrosis factor

WT = Wild-type

iNOS = Nitric oxide synthase

iTAM = Iron-retaining tumor-associated macrophage

2. FIGURE INDEX

3. TABLE INDEX

4. ABSTRACT

Over the last decade, the cell-cycle inhibitor p21 has been shown to sustain leukaemia propagation with two distinct mechanisms. On one hand, p21 was shown to be critical for maintaining increased self-renewal capacities of leukaemia stem cells. Indeed, the absence of p21 in leukaemia stem cells leads to their functional exhaustion, which results in loss of leukaemia transplantability in syngeneic mice. On the other hand, p21 expression is crucial for evading the surveillance mechanisms of the immune system, thus ensuring tumor growth. Specifically, lack of p21 in the leukemic microenvironment activates a potent $CD4^+$ T-cell mediated immunological response against tumor in syngeneic context (unpublished data from the host laboratory). To translate the observed p21-dependent anti-tumoral immunity into novel immune-therapies against cancer, underlying mechanisms needed to be unrevealed.

In my thesis work, I dissected the cellular bases of the p21-dependent anti-tumor immunity. I disclosed a crucial role of the $p21^{-/-}$ tumor microenvironment in triggering activation of an anti-tumor immunological response. In particular, for the first time I identified rare iron-loaded $CD68^+$ tumor-associated macrophages (iTAMs) in the p21-null context as key mediators of a potent immunological mechanisms of cancer clearance. By unravelling crucial players of the p21-dependent anti-tumor immunity, my work set the basis for the future design of novel anti-cancer vaccines. Such vaccines will grant more efficient and less toxic treatment for cancer patients.

To further transpose such immunological mechanism of cancer clearance in humans, the usage of a proper humanized mouse model is needed. Actually, humanized mice allow to study the interaction between human immune system and cancers of human origin. I generated $hCB-CD34^+$ NSG mice containing all the cellular components of human immunity. However, I showed that these mice are fully accessible to human tumor growth, demonstrat-

ing the inadequacy of hCB-CD34$^+$ NSG model in immuno-oncology. Thus, the development of a proper humanized mouse model to study p21-dependent anti-tumoral immune response in human context remains necessary.

5. INTRODUCTION

5.1 Role of the cell-cycle inhibitor p21 in cancer growth

5.1.1 p21 in cell-cycle regulation and DNA damage response. The cell-cycle inhibitor p21 was first discovered in the 1990's. It is a 165-amino acid protein that belongs to the CIP/kip family of cyclin-dependent kinase inhibitors[1]. p21 is able to bind CDK2 and negatively regulate the cyclin/CDK complex, inducing cell-cycle arrest in G1 phase[1]. Moreover, p21 has the ability to directly impede DNA replication by binding the polymerase co-factor PCNA (proliferating cell nuclear antigen)[2]. In this way, p21 can directly disrupt the interaction of PCNA with the DNA molecule, which further leads to a halt in DNA replication[2].

Apart from its pivotal role in regulation of cell-cycle, p21 has important functions in various cellular processes such as apoptosis, cell differentiation and transcriptional regulation[1]. p21 is recognized as a downstream effector of p53 in response to DNA damage[3]. Upon diverse cellular stresses, the upregulation of p53 leads to transcriptional activation of p21, which can further lead to G1 cell-cycle arrest, or activation of senescence or apoptosis[4].

5.1.2 Dual role of p21 in cancer. The association of p21 with cancer has been extensively studied in the last two decades. Initial studies unrevealed its role as a tumor-suppressor, since deletion of p21 in mice expressing a mutant form of p53 resulted in accelerated development of tumors[5]. In addition, it was shown that aged p21-deficient mice (>16 months) develop spontaneous sarcomas at higher frequency than wild-type mice, though with much longer latency then in mice lacking other tumor-suppressor genes, such as p53 and *ATM*[6], suggesting that the lack of p21 *per se* is not sufficient to promote tumor formation[7]. Other studies, however, showed that mice lacking p21 are not more tumor-prone than wild type mice, and that previous observations of increased spontaneous tumorigenesis in aged p21-deficient mice could be due to macrophage hyperactivation[8].

On the other hand, p21 can exhibit oncogenic activities[9]. Upregulation of p21 is often observed in many human cancers, and its overexpression positively correlates with poor prognosis[7]. It has been shown that in p53-deficient or p53-haploinsufficient mice, lack of p21 inhibits development of spontaneous lymphomas[10]. Moreover, recent studies have shown that p21 may promote tumor development through non-cell autonomous mechanisms. In particular, p21 expression in myeloid-derived suppressor cells (MDSCs) facilitates their recruitment in growing tumors (by upregulating CX3CR1 expression), thus conferring resistance to anti-tumor immune mechanisms[11].

Considering its dual role in malignancies, manipulation of p21 expression, either in cancer or tumor-infiltrating cells, may represent a novel anti-cancer strategy.

5.1.3 p21 and the regulation of self-renewal in leukaemia stem cells. Normal stem cells (SCs) are hallmarked by their ability to differentiate and self-renew. Self-renewal is a process by which SCs divide maintaining undifferentiated state and preserving SC pool[12]. Under physiological conditions, regulation of self-renewal is strictly controlled by both intrinsic and extrinsic cellular mechanisms. Diverse developmental pathways (such as Wnt, Notch and Hedgehog), as well as pathways involved in the regulation of cell survival and cell-cycle (p53, Bmi-1 and CDKi) represent crucial intrinsic mechanisms that regulate SC self-renewal[12,13].

Differentiation and self-renewal are achieved by normal SCs through a single mitotic division, so-called asymmetric division, which generate one SC and one committed cell (progenitor)[13,14]. Normal SCs divide limited numbers of times, and they functionally exhaust due to intrinsic regulation of self-renewal[13]. The asymmetric mode of division is imposed by functional p53[14]. In normal SCs, p21 is not epistatic to p53 and, following DNA damage, p53 expression is downregulated and p21 up-regulated, allowing SCs entering a symmetric self-renewing divisions[15]. In mammary tumors, cancer SCs (CSCs) undergo unlimited self-

renewing divisions, with a predominantly symmetric modality of division[14], while in myeloid leukaemias, leukaemia SCs (LSCs) and p21 increased-expression leads to extended self-renewal[16], suggesting that loss of p53 and p21 up-regulation contribute to the expansion of the pool of transformed SCs in tumors[13] (Figure 1).
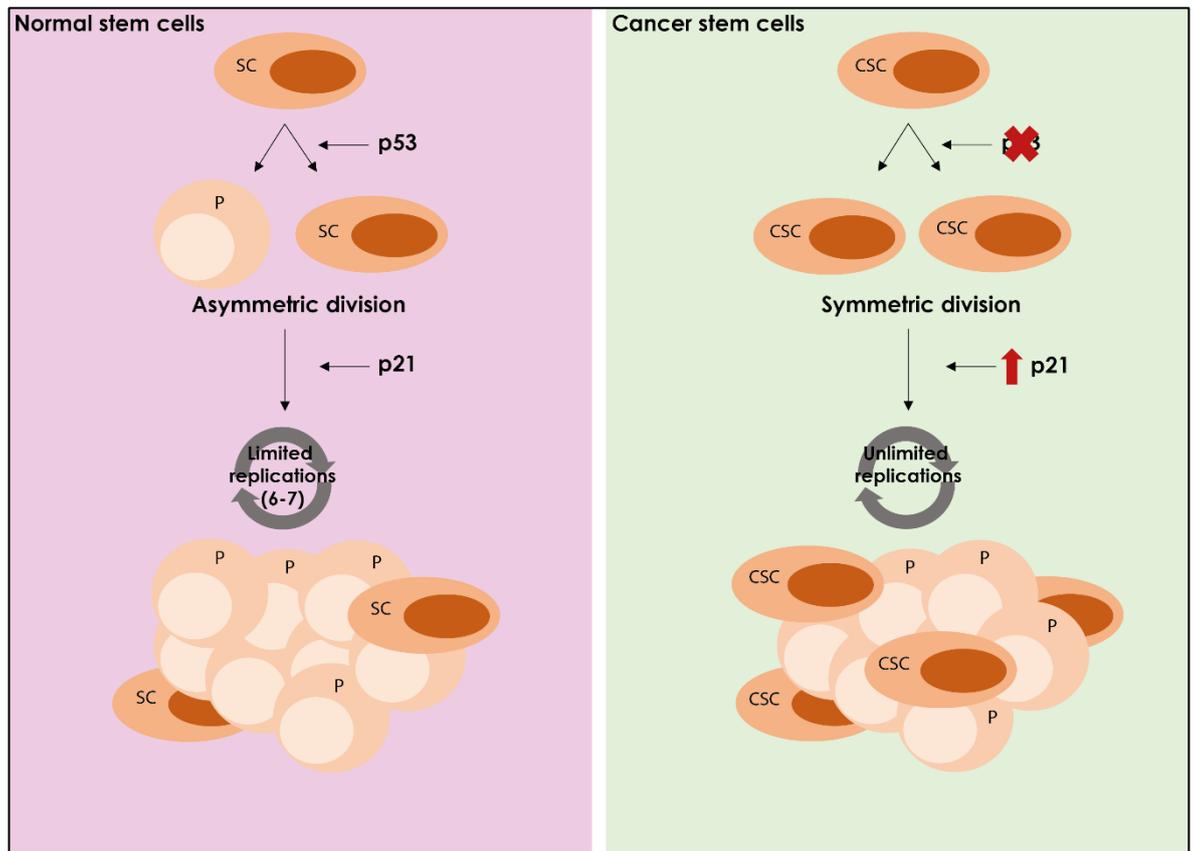
Figure 1. Regulation of normal and cancer SC self-renewal. Asymmetric mode of division of normal SCs is controlled by p53 and their self-renewal capacity is perpetuated by p21. By this mechanism, normal SCs undergo limited number of cell divisions, after which they functionally exhaust. On the contrary, CSCs divide symmetrically, due to the loss of p53, and upregulation of p21 results in unlimited self-renewal capacity (Adapted from Verga Falzacappa, MV. *FEBS J.* 2012).

In hematopoietic SCs (HSCs), self-renewal was shown to be tightly controlled by CIP/Kip family members of CDKi, p21, p27 and p57[17–20]. The role of p21 in self-renewal regulation of leukaemia SCs (LSCs) in mice has been disclosed by Viale et al. almost a decade ago, using PML-RAR knock in mice[21] backcrossed either in the wild type or p21 knock out C57BL6 backgrounds[16]. PML-RAR is the initiating oncogene of human acute promyelocytic leukaemia (APL), a subtype of acute myeloid leukaemia (AML)[21]. PML-RAR expression, as well as AML1-ETO (another AML-associated oncogene) induces DNA damage in HSCs

and activates a p53-independent and p21-dependent response, resulting in the maintenance of the pool of LSCs[16]. Expression of AML1-ETO and PML-RAR lead to accumulation of DNA damage in hematopoietic SCs, which increases significantly in the absence of p21. Strikingly, AML1-ETO failed to induce leukaemias in p21$^{-/-}$ mice[16]. p21$^{-/-}$ PML-RAR knock in mice, instead, developed APL with comparable latency and frequency as control mice. However, the p21$^{-/-}$ APLs were not transplantable in syngeneic recipients[16]. In light of this evidence, the authors postulated that the loss of p21 induces LSCs to hyperproliferate and accumulate massive DNA damage, resulting in their functional exhaustion[16].

5.2 Cell-extrinsic effects of p21 in cancer growth

5.2.1 p21 expression in AML and the regulation of the host's immune system. The increased replicative potential of LSCs was shown to be governed by constitutive activation of p21[16]. Absence of p21 in LSCs led to the exhaustion of their self-renewal and loss of transplantability in syngeneic mice. Strikingly, preliminary data of my host lab demonstrated that immune-deficient mice or syngeneic recipients after γ-irradiation, however, are completely permissive to the growth of p21$^{-/-}$ AMLs (both PML-RAR and AML1-ETO) (Verga Falzacappa, MV. *et al.* preliminary data). Notably, transplantability of p21$^{-/-}$ AMLs in immune-compromised hosts was shown not to be due to facilitated homing of leukaemia cells in immune-compromised recipients, nor to higher susceptibility of immune-deficient mice to the growth of wild type leukaemia (Verga Falzacappa, MV. *et al.* preliminary data), suggesting the involvement of cell-extrinsic mechanisms in the clearance of p21$^{-/-}$ leukaemias, and that the immune-competent host activates an immunological response specific to p21$^{-/-}$ leukaemia.

5.2.2 Cytotoxic CD4^{+} T cells mediate a p21-dependent anti-tumoral immune response against leukaemia cells.

Experiments of leukaemia transplantation in different immune-deficient mouse models (selectively depleted for specific cellular compartments of the immune system) showed that cytotoxic CD4^{+} T cells are responsible for the clearance of p21^{-/-} leukaemias in syngeneic host (Verga Falzacappa, MV. *et al.* preliminary data). Most importantly, a protective CD4^{+} T-cell population can be transferred *in vivo* in order to vaccinate immune-deficient mice (RAG1) against leukaemia development. A protocol to prime CD4^{+} T cells in syngeneic host using p21^{-/-} leukaemia was established: immune-competent mice are exposed to p21^{-/-} leukaemia for 15 days, after which CD4^{+} T cells are isolated from the spleen of these mice. The adoptive transfer of the isolated CD4^{+} T cells into immune-deficient RAG1 mice prevents growth of different clones of p21^{-/-} leukaemia, as well as AMLs of different origin (AMLs expressing the AML-associated NPMc or FLIT3 mutations) (Figure 2) (Verga Falzacappa, MV. *et al.* preliminary data). On the other hand, unprimed CD4^{+} T cells from syngeneic mice were shown not to be protective against leukaemia upon adoptive transfer in immune-compromised recipients (Verga Falzacappa, MV. *et al.* preliminary data).
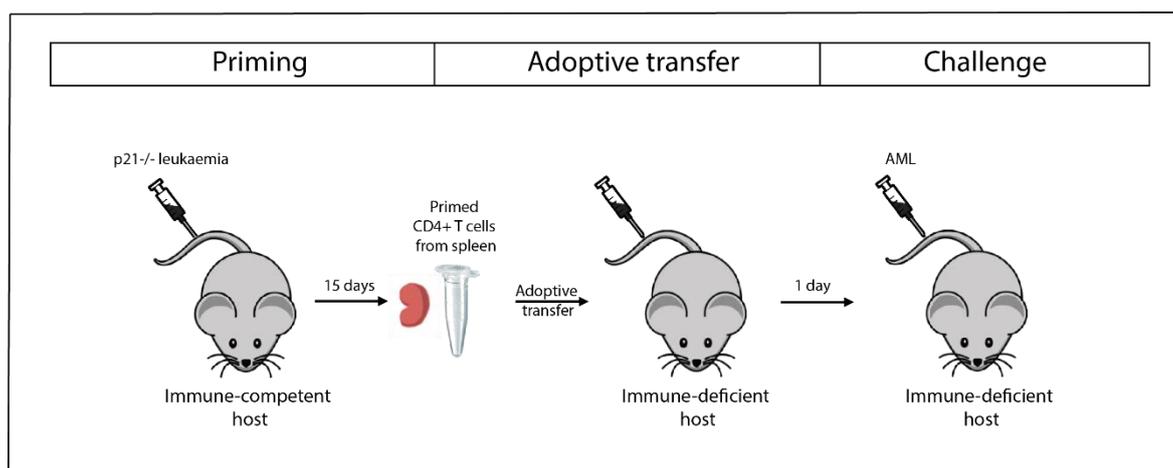
Figure 2. Generation of protective CD4^{+} T cells and their adoptive transfer in immune-deficient recipients. Immune-competent mice are exposed to p21^{-/-} leukaemia for 15 days. Consequently, primed CD4^{+} T cells are isolated from spleens of these mice and transferred in immune-deficient recipients, which are challenged the next day with AML. Anti-tumoral effect of CD4^{+} T cells primed with p21^{-/-} leukaemia is observed against AMLs in general.

5.2.3 The anti-leukaemia T-cell mediated immune response to p21^{-/-} leukaemias is MHC II dependent. T-cell mediated immune response is triggered by coordinated interactions of different molecules on T cells and professional antigen presenting cells (APCs). T cells can recognize antigens of infectious agents presented by the major histocompatibility complex (MHC) on APC through T-cell receptor (TCR)-MHC interactions[22]. Specifically, CD4^{+} T cells are activated by antigen-presentation via class II molecules of the major histocompatibility complex[22]. Preliminary data of my host lab showed that the activation of anti-leukemic T-cell mediated immune response triggered by the p21^{-/-} leukaemias depends on MHC II (Insinga, A. *et al.* preliminary data). Actually, *in vitro* analyses of T-cell proliferation showed that CD4^{+} T cells proliferate in the presence of p21^{-/-} leukaemia (Insinga, A. *et al.* preliminary data). However, the proliferative effect is halted by administration of anti-MHC II blocking antibody (Insinga, A. *et al.* preliminary data). Moreover, p21^{-/-} leukaemias, when depleted of MHC II^{+} cells, re-acquire the ability to propagate in immune-competent recipients (Insinga, A. *et al.* preliminary data). This evidence shed the light on an antigen-presenting cell being key mediator of CD4^{+} T-cell immunological response against leukaemia in a p21-dependent manner.

5.2.4 Lack of p21 expression in normal residual splenocytes impedes AML propagation.
Priming of CD4^{+} T cells by AMLs was performed transplanting cell preparations from the spleen of p21^{-/-} leukemic mice. p21^{-/-} leukemic spleens comprise of infiltrating p21^{-/-} leukemic blasts and residual cells of the non-leukemic p21^{-/-} splenic environment[16], suggesting that the normal cellular components of the p21^{-/-} spleen, rather than the p21^{-/-} blasts themselves, might be also involved in the anti-leukemic immunological response. To this end, in my host lab, it has been investigated whether the observed p21-dependent immune response to AML could also be achieved in the presence of WT leukemic blasts upon exposure to a p21^{-/-} splenic environment. Leukaemias obtained in WT C57BL6 mice ("WT leukaemias")

showed similar growth rates (in terms of latency and frequency of engraftments) upon transplantation in WT or p21^t C57BL6 mice (Verga Falzacappa, MV. *et al.* preliminary data). However, WT leukaemias grown in p21$^{-/-}$ recipient showed markedly reduced growth rates when re-transplanted in WT syngeneic recipients, in terms of survival rate of injected mice (see also paragraph 7.1.1). Thus, WT leukaemias exposed to the p21$^{-/-}$ environment "mimic" the behaviour of p21$^{-/-}$ leukaemias when re-transplanted in WT syngeneic host. These observations implied that the lack of p21 expression in the normal p21$^{-/-}$ splenocytes, rather than in the leukemic blast *per se*, contribute significantly, or is sufficient for the activation of a T-cell mediated immunological response against leukaemia (Figure 3). The demonstration that p21$^{-/-}$ splenocytes play a crucial role in mounting an anti-leukaemia immune response raises the question of how p21$^{-/-}$ mice develop leukaemia in the first place. One of the possible explanations is that despite the presence of anti-leukemic p21$^{-/-}$ splenocytes, the T-cell compartment of p21$^{-/-}$ mice is defective (as demonstrated in other studies)[23], thus not able to mount an anti-leukemic response.
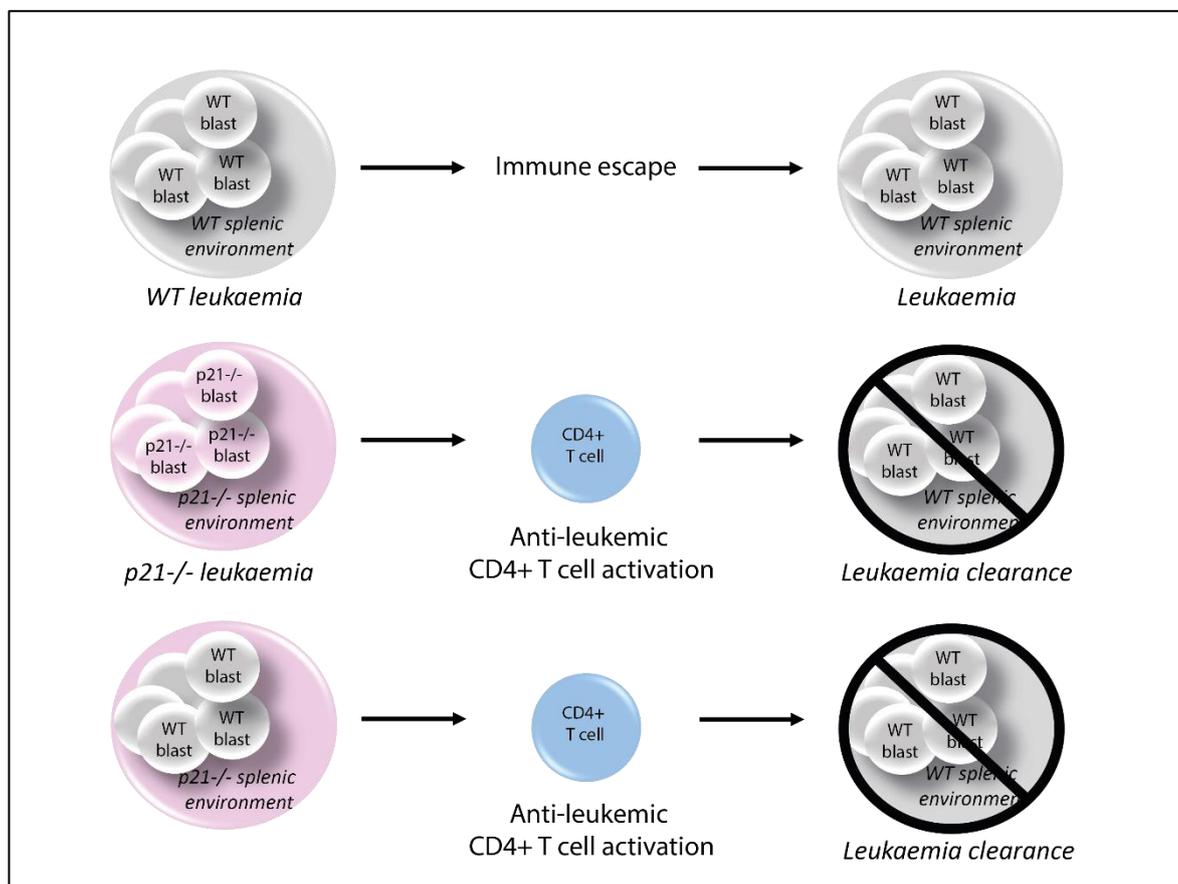
Figure 3. p21 expression in TME inhibits activation of anti-leukemic CD4$^+$ T-cell response. Syngeneic recipients transplanted with PRKi leukaemia succumb to disease. On the other hand, the growth of p21$^{-/-}$ leukaemia is suppressed in syngeneic mice due to the activation of a specific CD4$^+$ T cell population. The same anti-tumoral effect can be observed upon re-transplantation of PRKi leukaemia previously exposed to p21$^{-/-}$ environment.

5.2.5 Breast cancer and p21-dependent T-cell mediated immune responses. In my host lab, a p21-dependent cancer clearance, analogous to the one revealed in leukaemia, has also been observed in breast cancer, using transgenic mice overexpressing the breast-cancer specific ErbB2 oncogene (Insinga, A. *et al.* preliminary data). As observed with leukaemias, WT and p21$^{-/-}$ mice expressing the ErbB2 transgene develop breast cancers with similar latency and penetrance. However, ErbB2 tumors developed in p21$^{-/-}$ mice (p21$^{-/-}$ ErbB2 tumors) do not grow upon re-transplantation in WT syngeneic recipients, while they grow when transplanted in immune-deficient hosts (Insinga, A. *et al.* preliminary data). CD4$^+$ T cells primed *in vitro* with p21$^{-/-}$ ErbB2 tumors, but not naïve T cells, proliferate *in vitro* in the presence of either p21$^{-/-}$ or WT breast cancers (Insinga, A. *et al.* preliminary data). Moreover, the proliferation is completely abolished *in vitro* upon administration of anti-MHC II blocking antibody (Insinga, A. *et al.* preliminary data). Taken together, these data strongly support the evidence obtained in leukaemia, implying the existence of a p21-dependent anti-tumoral immune response. Additionally, they suggest that the p21-dependent cancer clearance is not tumor specific, but rather a broad immunological response against malignancy.

5.3 Cancer and autoimmunity

5.3.1 Mechanisms of autoimmunity: pro- and anti-tumoral functions. The immune system is a finely balanced network able to maintain immune homeostasis under normal physiological conditions. However, under certain conditions, such as cancer or autoimmunity, the immune system can either under or over-react, respectively. Malignant cells often camouflage

themselves expressing altered self- antigens to become unrecognizable to the immune system[24]. On the other hand, deregulation of mechanisms controlling immune tolerance to "self" antigens, results in break of self-tolerance and leads to development of autoimmune diseases[25].

Autoimmune diseases and immune-suppressive treatments may allow for tumor development[24–26]. For example, it has been observed that patients with rheumatoid arthritis have increased risk of lymphomas and lung cancer[27]. On the other side, immune-therapies against different types of cancer often correlate with the break of immune-tolerance and consequent autoimmune responses[24,28,29]. Indeed, emerging evidence suggests that development of autoimmunity during cancer treatment correlates with inhibition of tumor growth. It has been reported that patients with metastatic melanoma treated with antibodies against immune-checkpoint inhibitors (anti-CTLA-4 antibodies) develop severe autoimmune diseases[30], which correlates with tumor regression. Another study also reported positive correlation between severe autoimmunity and immune response against metastatic melanoma, ovarian and renal cell carcinoma[31].

Accumulating evidence suggests a tight association between cancer and autoimmunity, indicating that the manipulation of immune-tolerance mechanisms might be used to develop novel strategies or implement already used cancer treatments.

5.3.2 p21 and autoimmunity. p21 may affect multiple processes of the immune system. Deregulation of cell-cycle was shown to cause break of self-tolerance and associated autoimmune disorders[32]. In humans, it has been demonstrated that mutations in p21 and other genes such as HLA class I and II are associated with the development of systemic lupus erythematosus (SLE)[33,34]. Due to defective apoptosis, SLE patients develop anti-nuclear antibodies, followed by expansion of inflammatory cells that attack multiple organ systems, leading to overt disease and eventually death[35].

Studies in mice also demonstrated a role of p21 as a suppressor of autoimmunity[23,36]. It has been shown that in mice of mixed genetic background, deletion of p21 led to the development of severe and lethal lupus-like autoimmunity[36]. Characteristics of lupus, such as splenomegaly, lymphadenopathy, glomerulonephritis, T-cell accumulation and high levels of anti-DNA antibodies were observed in these mice[36]. The extreme disease outcome was associated to the mixed genetic background of these mice that enhanced the effect of p21 deletion[36]. Actually, p21-deficient mice of pure genetic background develop normally and over time show a mild loss of tolerance to DNA and a moderate, yet not lethal, lupus-like phenotype[23].

5.4 Tumor microenvironment: a critical accomplice in tumorigenesis

Evidence summarized above suggests that p21 plays a critical role in the regulation of immunity, and, in particular, in the regulation of the host response to the emergence and expansion of tumor cells.

The interaction between cancer cells and cells of the immune system in the tumor microenvironment influences significantly all steps of tumorigenesis, including tumor initiation, progression and metastasis[37]. The tumor microenvironment (TME) is formed and dominated by the tumor itself, which dictates molecular and cellular events in the surrounding tissue[38]. Cancer cells form TME by attaching to the extracellular matrix (ECM), thus becoming competent for interactions with other cells, such as neutrophils, macrophages (tumor-associated macrophages or TAMs), fibroblasts (cancer-associated fibroblasts or CAFs), myeloid-derived suppressor cells (MDSCs), dendritic cells (DCs), B and T cells, natural killer cells (NK) [38–41] (Figure 4). Such intercellular interactions are driven or regulated by a complex network of soluble factors, including pro-inflammatory cytokines, chemokines or growth factors, which may also induce inflammation or stimulate cancer cell growth[39]. During initial stages of cancer formation, immune cells are recruited to the tumor site in response to tumor-

derived signals. However, their anti-cancer function is often downregulated, therefore allowing for immune-evasion and tumor progression[38,40,41]. For example, TAMs present in TME inhibit lymphocyte effector functions by producing immune-suppressive cytokines such as IL-10[42]. Regulatory T-cells and MDSCs are expanded in TME and downregulate effector T cells and antigen-presenting cell (APC) functions[43,44].

Taking into consideration the complexity of TME and its critical role in tumorigenesis, development of novel therapeutic strategies to target and modify TME will be of great importance to effectively treat malignant diseases.
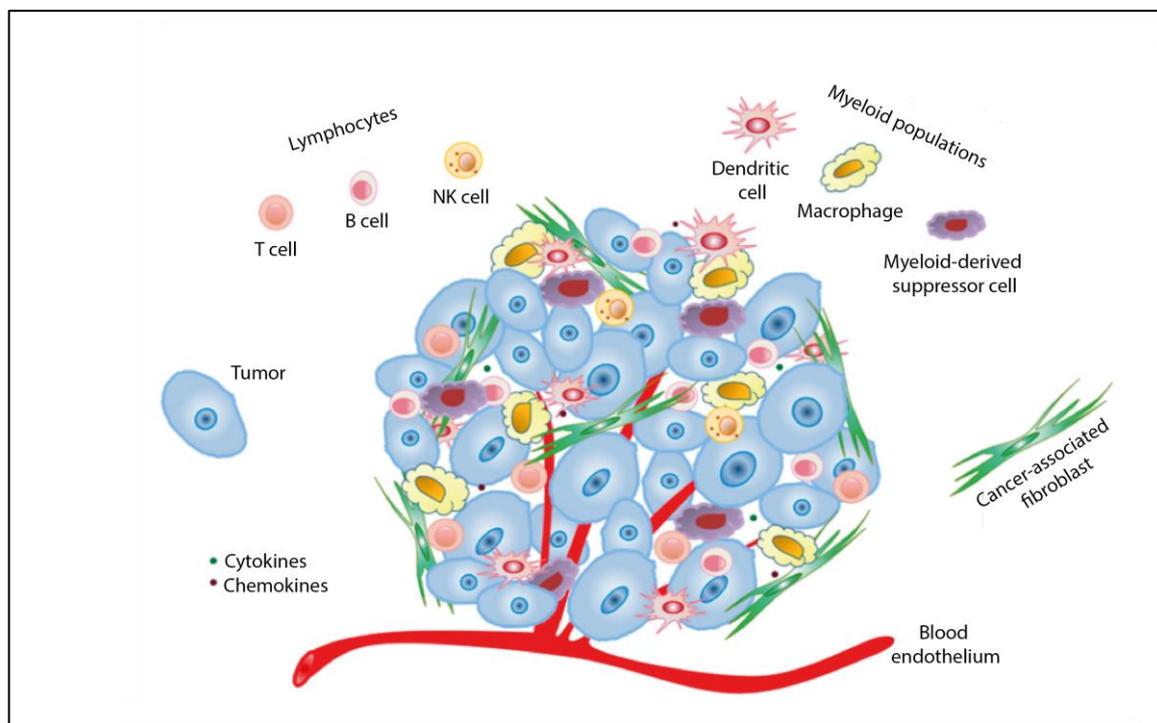
Figure 4. Organization of tumor microenvironment in solid tumors. Tumor microenvironment is formed by malignant cells that closely interact with extracellular matrix and other cells of both innate and adaptive immunity. This interaction is achieved either by cell-cell contact, or by secretion of diverse cytokines and chemokines that support tumor growth (Image adapted from Cui, Y et al. *Int. J. Mol. Sci.* 2016).

5.5 Immune cells of the tumor microenvironment

TME comprises of tumor stroma, blood vessels, infiltrating inflammatory cells and a variety of associated tissue cells. Both adaptive and innate immune cells, such as T cells, B cells,

dendritic cells (DCs), macrophages, and natural killer (NK) cells can be found in TME. Most immune cells of the TME inhibit anti-tumor immunity and promote tumor growth and progression[38,40]. In other cases, specific tumor-infiltrating immune cells (i.e. cytotoxic T lymphocytes) exert anti-tumor effects, and can be regarded as an attempt of host's immune response to react to slow tumor progression ("immune-surveillance")[39,45]. However, the pro-tumoral effects of the TME exceed consistently its anti-tumoral effects, resulting in tumor escape and progression.

In a variety of tumors, the majority of infiltrating inflammatory cells are $CD4^+$ and $CD8^+$ tumor-infiltrating lymphocytes (TILs)[38,46]. TILs can recognize specific tumor-associated antigens, however their effector function is often inhibited by other immune cells present in TME (such as regulatory T cells or TAMs), rendering them defective in supressing tumor growth[38].

A crucial portion of $CD4^+$ T cells present in TME are $CD4^+CD25^+Foxp3^+$ cells known as regulatory T cells (T-regs)[40,46]. Under physiological conditions, T-regs have a critical role in maintaining homeostasis of cytotoxic lymphocytes. In cancer, T-regs have immune-suppressive role and they often block the proliferation of cytotoxic T cells in TME either by direct contact or secretion of specific inhibitory cytokines (such as IL-10 and TGF-β)[38,44]. These cells also interfere with tumor-associated antigen-presentation by downregulating co-stimulatory molecules on DCs[44].

Another type of cells with immune-suppressive function found in TME is MDSCs[46,47]. They originate from the common myeloid progenitor in the bone marrow and often have a direct inhibitory effect on cytotoxic lymphocytes[47]. They are also known to impede M1 macrophage polarization[48], antigen-presentation by DC[43], and NK cell cytotoxicity[49].

Solid tumors are also infiltrated with macrophages, known as TAMs. TAMs often perform suppressive functions in TME by releasing inhibitory cytokines such as IL-10, prostaglandins and ROS[38,40,41]. In response to diverse microenvironmental stimuli, macrophages can

be polarized towards different functional phenotypes (see paragraph 5.5.1). Polarization of macrophages significantly impacts tumorigenesis. Macrophages activated in a classical fashion are polarized towards M1 phenotype and they may counteract tumor growth[50,51], while alternatively activated M2 macrophages often have a pro-tumoral role[42,52]. In fact, in a variety of human tumors, infiltrated macrophages are associated with M2 phenotype and their presence in TME negatively correlates with patient's survival[42]. It has been suggested that hypoxic TME in solid tumors is one of key factors that induces TAM polarization by up-regulating M2-related genes[53–55]. Other than inhibiting lymphocyte effector function, TAMs are also shown to be responsible for tumor entry in the vasculature[56,57], allowing for tumor dissemination.

5.5.1 Tumor-associated macrophages: dual role in cancer

5.5.1.1 M1 macrophage polarization and the pro-inflammatory phenotype. Macrophages are highly heterogeneous immune cells that can be found in almost all tissues. Their crucial role in tissue development, immune response to pathogens, iron metabolism and maintenance of tissue homeostasis is widely known[50,51]. They can undergo differentiation into various functional phenotypes depending on a variety of different environmental signals[51]. Conventionally, macrophages can be polarized either toward a pro-inflammatory, classically activated M1 phenotype, or to an anti-inflammatory, alternatively activated M2 phenotype[51,58,59]. Yet, accumulating evidence suggests that M1 and M2 phenotypes represent two extremes of a wide range of macrophage activation with intermediate M1/M2 phenotypes[59,60].

In TME, macrophages often represent the majority of the infiltrating leukocytes[61,62]. Most of TAMs originate from bone marrow-derived circulating monocytes[62,63]. Circulating monocytes are recruited from the peripheral blood to TME where they differentiate into TAMs in response to diverse cytokines, chemokines and growth factors released by tumor cells or

the TME[62]. TAMs are considered as a "double-edged sword" since they can either halt tumor progression[64,65] or promote tumor growth[52,61]. It has been initially suggested that in different types of tumors TAMs expressed the M2-like phenotype[52]. However, it is now clear that the TAM compartment in TME comprises of diverse populations with specific functions[60].

Macrophages can be polarized towards M1 pro-inflammatory phenotype in the presence of IFN-γ alone or in combination with microbial products (i.e. LPS) or cytokines (i.e. TNF)[66] (Figure 5). Activated M1 macrophages are characterized by high antigen-presenting capacity and secretion of pro-inflammatory cytokines such as IL-6, IL-12 and IL-23 and TNF[59,66]. M1-polarized macrophages are able to produce high amounts of toxic intermediates, such as iNOS and ROS which have strong microbicidal effect. They express high levels of MHC II molecules on their surface, CD68, and CD80 and CD86 co-stimulatory molecules[59]. Macrophages are crucial regulators of iron homeostasis and this characteristic is closely associated to their role in innate immunity[67]. Splenic and liver macrophages phagocyte senescent erythrocytes and sequester iron, that is then either stored intracellularly by ferritin, or exported in the environment via ferroportin[68]. M1-polarized macrophages are hallmarked by high accumulation of iron, due to increased levels of ferritin and low ferroportin expression[69,70]. Expression of genes involved in iron metabolism is either dependent on macrophage polarization or conversely, dictates the polarization state of macrophages[67].

M1-polarized TAMs present in TME were shown to be effective in suppressing tumor growth, either by activating components of the adaptive immune system or by directly killing tumor cells[64,65,71]. For example, the presence of M1 TAMs in patients with non-small cell lung cancer (NSCLC) was shown to positively correlate with patient's extended survival[72,73].

5.5.1.2 M2 macrophage polarization and anti-inflammatory phenotype. M2 polarized macrophages are so-called "alternatively activated macrophages" and they arise upon exposure to cytokines such as IL-4, IL-10 and IL-13[51,59,66] (Figure 5). They are known to mediate anti-inflammatory processes, immune regulation and tissue remodelling[59]. Mantovani and co-authors suggested that the M2 activated macrophage population can be divided into three well defined phenotypes. Exposure to IL-4 and IL-13 or immune complexes (IC) and agonists of TLR or IL-1R induces polarization to M2a or M2b phenotypes, respectively, both of which exhibit immune-modulatory functions[59,66]. IL-10 induces the M2c activation phenotype, which is involved in tissue remodelling and immune-suppression[59,66]. Phenotypically, M2-like macrophages are characterized by low expression of MHC II, high expression of IL-10, CD163, CD200R, CD206, arginase-1 and low expression of IL-12[66]. The production of iNOS and ROS is inhibited in M2 activated macrophages[52]. Comparing to M1 phenotype, M2 macrophages express more ferroportin and less ferritin, and thus have enhanced ability to release iron[69,70].

It has been suggested that most TAMs in TME are of the M2-polarized phenotype, with immune-suppressive and tumor-promoting functions. M2-like TAMs are usually located in hypoxic areas of the tumor, where they play an active role in tumor invasion and angiogenesis[55]. It has been shown that the presence of anti-inflammatory cytokines released by M2-TAMs such as IL-10, is closely associated with tumor progression. By releasing immune-suppressive cytokines, M2-like TAMs downregulate cytotoxic T-cell effector functions and induce expansion of T-regs that further inhibit anti-tumoral immunity[42]. In a variety of tumors, macrophage infiltration correlates with poor prognosis for patient's survival[42,62,74]. Due to strong evidence supporting their pro-tumoral role, M2 TAMs represent potential therapeutic targets in cancer treatment.
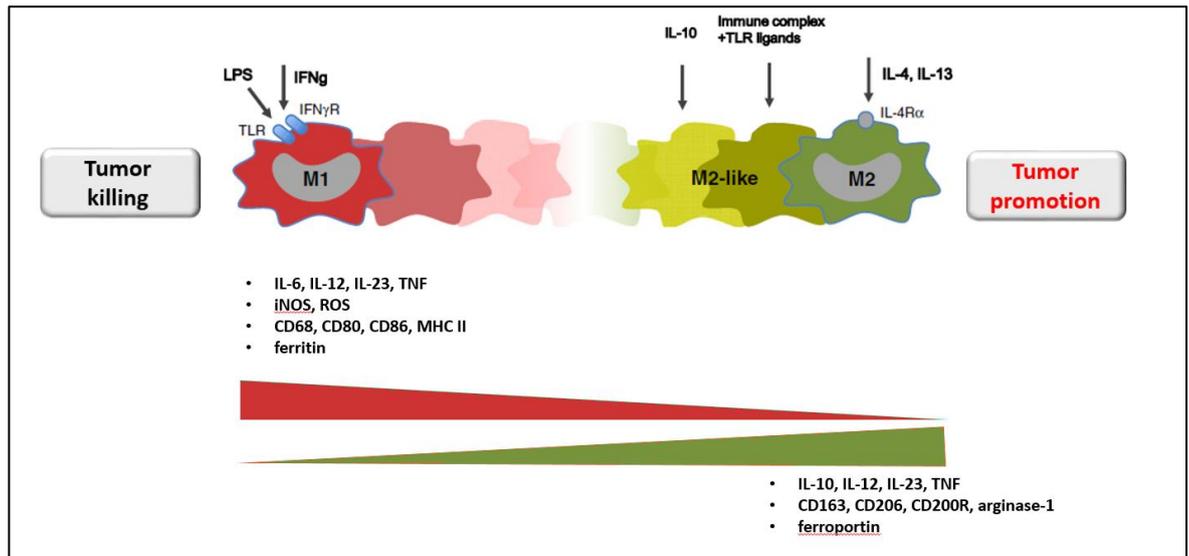
Figure 5. Polarization landscape of macrophages. Different phenotypes that macrophages can acquire depending on the environmental stimuli. Two extreme phenotypes are M1, stimulated by IFN-γ alone or in combination with microbial products such as LPS, and M2, induced by exposure to IL-10, IL.4 and IL-13, as well as to immune complexes and TLR ligands. Different gene expression profile of polarized macrophages describes their role either in halting tumor growth (M1) or promoting its progression (M2).

5.5.1.3 Other types of TAMs. Recent studies have reported other populations of TAMs that are able to either inhibit or promote tumor growth or progression. For example, macrophages that secrete IFN-γ were identified in mouse models of melanoma where they promoted tumor growth[75]. A recent study identified in cases of NSCLCa subpopulation of pro-inflammatory CD68^{+} iron-retaining TAMs (iTAMs) with anti-tumoral functions[76]. The authors demonstrated that in haemorrhagic areas of TME, red blood cells (RBCs) release heme and iron that are consequently up-taken by TAMs[76]. Heme and iron induce TAM reprogramming to a pro-inflammatory phenotype that negatively impacts tumor growth and progression[76].

5.6 Tumor microenvironment in haematological malignancies

In solid tumors, TME represents the environmental niche surrounding malignant cells. In case of haematological malignancies, even though cancer cells are not strictly encircled by all the environmental components, TME still exists and has a crucial impact on tumorigenesis. TME in leukaemias resides in the bone marrow (BM), blood vessels and secondary lymphoid organs such as the spleen[77]. Abnormalities in the BM niche severely affect normal haematopoiesis leading to the development of haematopoietic malignancies in both mice and humans[78]. The BM microenvironment in haematological cancers consist of complex network of cellular interactions and soluble factors. Different cell types can be found in the BM microenvironment of leukaemias, such as osteoclasts, osteoblasts, T and B cells, macrophages, and other cells of the immune system[79]. As in solid tumors, cells of BM microenvironment such as T-regs, MDSCs and TAMs often show immune-suppressive or tumor promoting function[80]. Even though there is evidence that anti-tumoral effector T cells can be found in TME of haematological malignancies such as myeloma, their effector function is often downregulated allowing for disease progression[81]. Although most of the studies legitimately pinpoint the BM niche as the TME in haematological tumors, the involvement of the spleen microenvironment in the development and progression of hematopoietic malignancies must also be considered. Spleen is a secondary lymphoid organ with important role in adaptive immune response. Diverse spectrum of immune cells, such as T and B lymphocytes, macrophages, NK cells and DCs can be found in spleen. As the BM, the spleen microenvironment has an impact on haematological malignancies. In fact, splenomegaly is often observed in patients with some types of leukaemia, such as T-ALL, as the result of infiltration of leukemic blasts at the late stages of disease[82]. In case of Notch1-induced T-cell acute lymphoblastic leukaemia (T-ALL), it has been demonstrated that microenvironmental cues from spleen had a promoting effect on dissemination of leukemic cells[83]. This suggested that spleen might be a more important environment for the initiation and early development

of a Notch1-induced T-ALL[83]. Moreover, a pro-tumoral function of the spleen microenvironment was observed in mouse models of chronic lymphocytic leukaemia, since selective depletion of splenic myeloid cell subpopulations such as TAMs delayed leukaemia progression[84].

The BM and spleen microenvironments represent specific niches that highly impact development and progression of haematological malignancies. Alteration of splenic and BM microenvironmental cellular components towards phenotypes that enhance anti-tumoral immunity could result in tumor clearance and thus is a promising way to treat haematopoietic cancers.

5.7 Humanized mouse models as a preclinical tool to study interactions between human immune system and cancer

The promising field of immune-oncology aims to study, use and manipulate immunity to recognize and eliminate cancer cells. In order to model complex interactions between the human immune system, human tumor cells and the TME, it is necessary to reproduce all these interactions in an *in vivo* context. Models of human tumors growing *in vivo* are well established since decades in many murine xenograft systems where human cancer cells or tumor biopsies are heterotransplanted into immune-deficient rodents. On the other hand, humanized mice, that carry a human immune system, have been developed over the past three decades[85,86]. The development of humanized mouse models relies on the use of immuno-deficient mice that allow engraftment of human hematopoietic stem cells (hHSCs) and tissues, followed by generation of a functional human immunity into the murine context[87]. Over the past years, different immune-deficient mouse strains have been developed and tested for hHSC and tissue engraftment and many steps forward have been made to obtain a

good level of engraftment of the human cells. Initially, CB17-scid mice were shown to support the engraftment of hHSCs only at low level due to the presence of murine immune barriers (i.e. NK cells)[88]. Consecutively, NOD-scid mice allowed good engraftment of hHSCs, but their relatively short life span and residual innate immunity were considerable limitations[89]. Finally, NOD-*scid*IL2Rgamma[null] (NSG) mice, that lack all the components of murine innate immunity and allow a highly efficient engraftment of human HSCs[90,91] became a gold standard platform to recapitulate the human immune system in mice[92].

The development of a complete human immune system in NSG mouse model can be achieved by transplantation of human peripheral blood leukocytes[93], human stem cells (originated from peripheral blood, cord blood or bone marrow) or bone marrow, fetal liver and thymus along with autologous fetal liver HSCs[90]. However, recapitulation of human immunity in NSG mice is often followed by development of graft-versus-host disease[94] or non-functional human T-cell compartment in these mice[95]. Despite their caveats, humanized NSG mice were proposed to be a great tool to study infectious diseases, autoimmunity and drug metabolism, due to the existence of at least partially functional human immune system. Yet, the remaining limitations of this model still need to be surpassed. One of the major obstacles is the poor organization of secondary lymphoid structures that negatively impacts humoral response[86]. Nevertheless, a recent study demonstrated that intrahepatic injection of human cord blood hematopoietic stem and progenitor cells (HSPCs) in sublethally irradiated newborn triple transgenic NSG (SGM3) mice expressing human stem cell factor, granulocyte colony-stimulating factor and IL-3, resulted in complete reconstitution of haematopoiesis in these mice[96]. T-cell compartment reconstituted in these mice was demonstrated to be fully functional to human alloantigens[96]. Moreover, human T cells failed to induce GVHD upon adoptive transfer into sublethally irradiated secondary NSG recipients[96]. Despite all the efforts to develop an excellent mouse model that carries functional human immunity, still an optimal humanized mouse for immune-oncology studies has not been generated and further progress in the field is necessary.

5.8 Aims of the project

My project stemmed from the hypothesis that the cell-cycle inhibitor p21 inhibits the anti-leukemic activities of the TME. This is based on the preliminary observation that transplantation of leukaemia cells previously grown in $p21^{-/-}$ mice, activate anti-leukemic $CD4^{+}$ T cells. My specific goal was to identify the peculiar TME cellular-components that, in the p21-null context, mediate activation of anti-leukemic T cells. Specifically: i) first, I set-up experiments to definitively exclude a role of $p21^{-/-}$ leukemic blasts in mounting the anti-leukaemia immune response; ii) I then analysed the composition and functional status of the $p21^{-/-}$ spleen TME; iii) I searched for the specific TME cellular component involved in anti-leukaemia responses; iv) I investigated whether the observed phenomenon is strain-specific, analysing its reproducibility in an another mouse strain;

6. MATERIALS AND METHODS

6.1. Mouse strains

Animals were housed in the animal facility at European Institute of Oncology, in pathogen-free conditions. All the procedures related to mouse use have been communicated and approved by the Italian Ministry of Health.

C57Bl6 mice were purchased from Charles River Laboratories. FVB/Hsd (FVB) animals were purchased from Harland Laboratories. $p21^{-/-}$ C57Bl6, $p21^{-/-}$ FVB and NOD-*sci-d*IL2Rgamma^{null} (NSG) mice were provided from breeding area of the mouse facility at European Institute of Oncology. PML-RAR knock-in mice (PRKi) were provided by T. J. Ley and backcrossed in the C57BL6 background. These mice express the PML-RARα oncogene in stem and early myeloid cells under control of murine cathepsin G promoter. Murine APL develops spontaneously in these mice with 70% penetrance at 6-16 months of age (median 10 months) and resembles the human APL. $p21^{-/-}$ PRKi mice were generated in the breeding area of the mouse facility at IEO, by mating PRKi and $p21^{-/-}$ C57Bl6 mice. These mice develop spontaneous leukaemia at the age of 8-16 months (40% penetrance).

6.2. *In vivo* procedures

6.2.1 Leukaemia transplantation. Leukemic spleens of PRKi and $p21^{-/-}$ PRKi mice were used as a source of leukemic blasts and were transplantated in 7-12 weeks old WT and $p21^{-/-}$ C57Bl6 recipients. 1×10^6 cells per mouse was injected in the caudal vein. Upon transplantation, mice were followed for the disease development by controlling the haematological parameters (bleeding via tail vein was performed weekly). Mice have been also followed every 2-3 days to evaluate any sign of distress, such as pale extremities, curved posture, reluctance in motion. At the onset of the disease, mice were euthanized (using CO_2) and

leukemic spleens were collected and consecutively used in re-transplantation experiments in syngeneic recipients.

6.2.2 Tumor-stimulated macrophages. In order to challenge macrophages *in vivo* with leukaemia, WT and p21$^{-/-}$ C57Bl6 mice 7-12 weeks old were intravenously injected with $5x10^6$ PRKi leukaemia cells/mouse. Mice were sacrificed prior leukemic blast infiltration in the spleen, 8h, 24h, 48h and 7 days post leukaemia transplantation. Spleens of the mice were collected, processed to single-cell suspension and used in subsequent experiments.

6.2.3 DNA damage induction in vivo. WT C57Bl6 mice were irradiated 2, 4 or 6 Gy for induction of acute DNA damage or treated with N-ethyl-N-nitrosourea (ENU) (Sigma Aldrich, Cat. No N3385), as a source of chronic DNA damage. ENU was injected intraperitoneally once (50 mg/kg)[16]. The animals were sacrificed immediately after irradiation, or 5 and 10 days post ENU treatment, and their spleens were collected. Spleens were processed to single-cell suspension, followed by immunofluorescence staining.

6.2.4 DFO and hemin treatment in vivo. For iron depletion, deferoxamine mesylate salt DFO (Sigma Aldrich, Cat. No D9533) was used. WT and p21$^{-/-}$ C57Bl6 mice were injected intraperitoneally with a single dose of 100mg/kg DFO[97]. For iron overload, mice were treated with a single dose of 75mg/kg hemin (Sigma Aldrich, Cat. No H9039)[97]. Mice were sacrificed 15 hours post DFO or hemin treatment.

6.2.5 Blood smears and blood analysis. In the experiments where leukaemia formation was followed, mice were weekly bled via tail vein. Blood parameters such as white and red blood cells, haemoglobin, platelets, were analysed using haematoanalyzer (Beckman Coulter). Blood was also smeared on the glass slides and left to dry for 1-2h, after which Giemsa (Sigma Aldrich, Cat. No 51811-82-6) and May Grünwald (Sigma Aldrich, Cat. No MG500) staining was performed, according to manufacturer's protocol. After staining, slides were mounted with Eukitt (Bio-Optica, Cat. No 09-00501) and analysed using Upright Olympus BX 51 Full Manual Wide Field microscope.

6.3. Generation of MLL-AF9 leukaemia in FVB mouse strain

Lin$^-$ cells were FACS isolated from BM of WT and p21$^{-/-}$ FVB mice, 6-7 weeks old. In particular, total BM cells were extracted by crushing bones from posterior limbs and sternum. Total BM cells were layered onto density gradient (Histopaque® 1083, Sigma-Aldrich) and centrifuged at 1800 rpm, 45 minute at 16°C. After centrifugation, BM-mononuclear cells remain at the PBS-Histopaque® interface and can be collected. BM-MNC were incubated in blocking solution (PBS + 10% BSA + 10% Rat Serum) for 30 minutes at 4°C. Staining for Lin$^-$ was performed in PBS + 1% BSA, 1 hour at 4°C in the dark, using the following lineage antibodies (all purchased from eBioscience, Pe-Cy7-conjugated, at concentration 1:200): CD3, B220, Ter119, Mac, Gr1). Lin$^-$ cells were FACS sorted using (MoFlo Astrios, Beckman Coulter). After sorting, Lin- cells were plated in Retro-Nectin coated 6-well plates (300 000 cells/ml) in RPMI, 10% Fetal Bovine Serum (FBS Stem Cell), interleukin-3 1000x, interleukin-6 1000x, Stem Cell Factor (S-CF 100x), 100 U/ml penicillin/streptomycin, 2mM L-glutamine and incubated at 37°C overnight. Lin$^-$ cells were transduced by spinoculation with the retroviral vector expressing MLL-AF9 fusion protein which expresses Venus (green). Infected Lin$^-$ cells were then sorted and intravenously injected in FVB WT and p21$^{-/-}$ mice sub-lethally irradiated (4 Gy) 16 hours prior transplantation. MLL-AF9 leukaemia

develops in WT FVB recipients around 80 days post injection. Immunophenotype of the leukaemia was assessed by FACS analysis, using fluorochrome-conjugated antibodies against myeloid and lymphoid markers. Leukemic spleen of WT FVB mice was used for re-transplantation experiments.

6.4 Cell sorting and flow cytometry analysis

All the cells used for FACS analysis were first incubated in blocking solution for 30 minutes at 4°C, after which specific fluorochrome-conjugated antibodies were added to the staining solution (PBS, 1% BSA) in concentration 1:200, if not indicated diversely by the manufacturer. Cells were stained for 1h at 4°C in dark and consecutively analysed via FACS (BD FACSCantoII, FACSDiva Version 6.1.1 software).

For the experiments of macrophage activation, anti-CD11b (FITC-conjugated, eBioscience, Cat. No 11-0112-85), anti-Ly6G (PE-conjugated, eBioscience, Cat. No RB6-8C5), anti-Ly6C (APC-conjugated, BD Biosciences, Cat. No 560595) and anti-MHC II (Pe-Cy7-conjugated, eBioscience, Cat. No 25-5321-82) were used.

For the analysis of origin and physical distribution of macrophages in the spleen, following antibodies were used: anti-MARCO (PE-conjugated, LifeSpan Biosciences, Cat. No 108347), anti-CD206 (PE-conjugated, BioLegend, Cat. No 141705), anti-CD209b (APC-conjugated, Miltenyi Biotech, Cat. No 130-106-331), anti-Dectin-2 (FITC-conjugated, Miltenyi Biotech, Cat. No 130-103-011), anti-F4/80 (APC-conjugated, eBioscience, Cat. No 17-4801-82), anti-CD11b (PE-conjugated, eBioscience, Cat. No 12-0112-81), anti-CD169 (PE-conjugated, BioLegend, Cat. No 142403), anti-CD68 (Brilliant Violet 421-conjugated, BioLegend, Cat. No 137017). When using markers for intracellular staining (anti-CD68 and anti-CD206), Fixation/Permeabilization Solution Kit (BD Biosciences, Cat. No 554714) was used, according to manufacturer's protocol.

For *in vivo* transplantation experiments, CD11b$^+$ and CD11c$^+$ cell populations were isolated from spleens of WT and p21$^{-/-}$ C57Bl6 mice. Cell sorting was performed via magnetic isolation, using magnetic columns along with anti-mouse CD11b microbeads (Milteny Biotech, Cat. No 130-049-601) or anti-mouse CD11c Ultra Pure microbeads (Miltenyi Biotech, Cat. No 130-108-338), according to the manufacturer's protocol.

6.5 Production of BMDMs

Posterior limbs and sternum were collected from WT and p21$^{-/-}$ C57Bl6 mice. Bones were crushed, and total BM cells were collected. 1.5×10^6 total BM cells were plated in sterile 10cm Petri-dish in Macrophage-specific medium: Dulbecco's Modified Eagle Medium (DMEM), 20% Fetal Bovine Serum North American (FBS NA), 1% L-glutamine, 1% penicillin/streptomycin, 0.5% NaP, 0.1% β-mercaptoethanol, 30% L929 medium. Plates were incubated at 37°C for 6 days, after which differentiated macrophages were gently scraped from the plates and used for specific experiments.

6.5.1 IFN-γ and LPS stimulation. BMDMs were incubated with 150U/ml IFN-γ (Prepro-Tech, Cat. No 315-05) for 6 hours in culture medium previously described (see paragraph 6.5). After incubation, plates were washed with warm culture medium, and subsequently fresh medium containing 10ng/ml LPS (Sigma Aldrich, Cat. No L2630) was added. Stimulated BMDMs were collected 24h post LPS stimulation.

6.6 Immunohisctochemistry

Spleens of healthy or leukaemia-challenged WT and p21$^{-/-}$ C57Bl6 mice assigned to histological assessment were fixed in 4% paraformaldehyde overnight at 4°C. The next day the samples were washed in 70% ethanol and submitted to paraffin embedding using Diapath

automatic processator. 5um sections were stained with hemtoxilin/eosin. Consecutive slides were stained for specific antibodies, following this protocol: paraffin was removed with xylene and the sections were rehydrated in graded alcohol. Antigen retrieval was carried out using preheated target retrieval solution for 45 minutes. Tissue sections were stained with H_2O_2 for quenching of endogenous peroxidases, blocked with FBS in PBS for 60 minutes and incubated overnight with primary antibodies. The antibody binding was detected using a polymer detection kit (GAR-HRP and GAM-HRP, Microtech) followed by a diaminobenzidine chromogen reaction (Peroxidase substrate kit, DAB, SK-4100; Vector Lab). All sections were counterstained with Mayer's hematoxylin and visualized using a bright-field microscope.

Primary Ab	Species	Dilution	Code/Company
Monoclonal anti-CD68 (KP1)	Mouse	1:200	#ab955/Abcam
Polyclonal anti-Iba1	Rabbit	1:1000	#019-19741/Wako
Monoclonal Ki67 (SP6)	Rabbit	1:20	#MA514520 /ThermoFisher Scientific
Polyclonal anti-Bcl6	Rabbit	1:150	#4242/ Cell Signalling Technology
Monoclonal anti-CD3ε (D4V8L)	Rabbit	1:150	#99940/ Cell Signalling Technology
Monoclonal anti-CD4 (D7D2Z)	Rabbit	1:100	#25229/ Cell Signalling Technology
Monoclonal anti-CD8α (D4W2Z)	Rabbit	1:400	#98941/Cell Signalling Technology

Table 1. Primary antibodies used for immunohistochemistry

6.7 Prussian Blue staining (PERLS')

Detection of iron-loaded macrophages was performed on paraffin-embedded samples of WT and $p21^{-/-}$ spleens, previously collected from the mice under steady state or challenged with leukaemia. The Prussian Blue staining was performed using Perls' Kit (Bio-Optica, Cat. No # 04-180807), according to manufacturer's protocol.

Double staining of Fe-content and CD68 was performed as follows: CD68 immunostaining was performed first, after which the slides were dis-assembled and stained with Perls'.

6.8 Immunofluorescence

Cells were fixed in 2% formaldehyde and seeded in 24-well plates (1×10^6 cells/well) onto poly-lysine cover slips. Plates were left at 4°C overnight. The following day, fixation was performed with 4% paraformaldehyde for 4 minutes at RT. All further manipulations were performed at RT. After three-time washing with PBS, fixed cells were permeabilized with 0.1% Triton-x100 in PBS for 10 minutes. Blocking was performed in PBS + 5% BSA for 30 minutes at RT, followed by incubation with the primary anti-γ-H2AX-Phosphorylated Alexa 647–conjugated antibody (BioLegend) (1:200) for 1 hour. Detection was performed using anti-goat Cy3-conjugated (Invitrogen). After staining with the primary antibody, blocking was performed in PBS + 5% BSA + IgG (250x) for 15 minutes, after which staining with anti-CD11b FITC-conjugated antibody (eBioscience) (1:200) was performed at RT for 1 hour. Following, DAPI (4,6 diamidino-2-phenylindole; Sigma-Aldrich) was used to stain the nuclei for 10 minutes. Cover slips were then put on the slides and mounted with Mowioll (Calbiochem). Images were acquired using Image Wide Field Microscope (Upright Olympus BX 61).

6.9 RNA reverse transcription and qPCR

Total RNA was extracted from splenic macrophages (WT and p21$^{-/-}$) using Quick RNA Kit (Zymo Research, Cat. No R1050) according to manufacturer's protocol. 0.1-1µg of total RNA of each sample (quantified by ND1000 Spectrophotometer) was reverse transcribed using ImProm-II™ Reverse Transciptase kit (Promega) according to manufacturer's instructions. RNA was first incubated with random primers (0.5µg/reaction) at 75°C for 10 minutes and then chilled on ice, after which the following mix was added (per sample):

ImProm-II™ 5X reaction buffer	4 µl	
MgCl$_2$ 25mM	3.2 µl	
dNTPs (10mM each)	1 µl	
recombinant RNAse inhibitor	1 µl	
ImProm-II™ Reverse Transcriptase	1 µl	
Nuclease-free water	0.8 µl	

Reaction was then incubated at 42°C for 90 minutes, and then at 70°C for 10 minutes. cDNA was stored at -20°C. For mRNA expression, qPCR was performed using 10 ng of cDNA, 0.2 µM of both forward and reverse primers and 10 µl of FAST SYBER™ Green Master Mix, AmpliTaq® Fast DNA Polymerase (ThermoFisher) in a final volume of 20 µl per reaction in 96-well plate. Fluorescence accumulation during qPCR reaction was detected on CFX96 Touch™ Real-Time PCR Detection System (Biorad). The mRNA/cDNA abundance of each gene was calculated relative to the expression of a house-keeping gene, GAPDH (glycer-aldehyde-3-phosphatedehydrogenase). Primers used are listed in Table 2.

Gene of interest	Sequence
GAPDH	Fw 5'-CCCATTCTCGGCCTTGACTGT-3'
	Rev 5'-GTGGAGATTGTTGCCATCAACGA-3'
Tfr1	Fw 5'-CCCATGACGTTGAATTGAACCT-3'
	Rev 5'-GTAGTCTCCACGAGCGGAATA-3'
Hif1α	Fw 5'-CATGATGGCTCCCTTTTTCA-3'
	Rev 5'-GTCACCTGGTTGCTGCAATA-3'
TNFα	Fw 5'-TGCCTATGTCTCAGCCTCTTC-3'
	Rev 5'-GAGGCCATTTGGGAACTTCT-3'
HO1	Fw 5'-AGGCTAAGACCGCCTTCCT-3'
	Rev 5'-TGTGTTCCTCTGTCAGCATCA -3'
Ireg1	Fw 5'-TGTCAGCCTGCTGTTTGCAGGA-3'
	Rev 5'-TCTTGCAGCAACTGTGTCACCG-3'

Table 2. List of primers used for qPCR.

6.10 Humanization of NSG mice and propagation of hCB-CD34+ cells

hCB-CD34+ cells were purchased from Stem Cell Technologies (Cat. No 70008). The cells originate from human cord blood of mixed healthy donors. For NSG humanization, 400 000 cells per mouse were transplanted in sublethally irradiated (1 Gy) NSG mice, 6-8 weeks old. For hCB-CD34+ cell propagation, BM cells of already humanized NSG recipients were re-transplanted in sublethally irradiated (1 Gy) NSG recipients. BM cells were processed as previously described in paragraph 6.3.

6.11 *In vitro* assays

6.11.1 CD3/CD28 activation assay. 96-well plate was coated with 5µg/ml of anti-human anti-CD3 antibody (eBioscience, Cat. No 16-0037) for 2 hours at 37°C. Following, cells were prepared and added to the plate (150 000 cells/well). Immediately after, 2µg/ml of anti-human anti-CD28 antibody (eBioscience, Cat. No 16-0289) was added to each well and plate was incubated at 37°C for 4 days.

6.11.2 CFSE proliferation assay. Human T cells, isolated from the spleens of hCB-CD34+ NSG mice, were stained using CellTrace™ CFSE Proliferation kit (ThermoFisher, Cat. No C34554), according to manufacturer's protocol. 4 days post culture, proliferation of these cells was assessed via FACS.

6.12 Human AMLs

Two different primary human AMLs were used for transplantation experiments in hCB-CD34+ NSG mice. Human AMLs originate from IEO Biobank. hAML1 derived from a patient affected by an M4 AML, harbouring the translocation t(9;11). hAML2 is leukaemia

with normal karyotype, bearing mutations in NPM and FLT3 genes. These leukaemias were xenotransplanted once in NSG mice, and leukemic spleens of these mice were used further in the experiments. hCB-CD34$^+$ NSG mice or the control animals were transplanted with 1x10^6 hAML cells.

7. RESULTS

7.1 The lack of p21 expression by the TME allows immunological recognition and eradication of leukemic cells

7.1.1 WT leukaemias grown in the p21$^{-/-}$ TME have impaired ability to propagate in WT mice

The preliminary data of my host lab demonstrated that p21$^{-/-}$ leukemic spleen activates anti-leukemic CD4$^+$ T cells upon transplantation in syngeneic mice. This suggests that the p21$^{-/-}$ TME contributes to the immunological response against leukaemias in this experimental setting. Thus, to formally separate the contribution of p21$^{-/-}$ leukemic blasts from that of the p21$^{-/-}$ TME, we analysed the growth properties of WT leukaemias transplanted in p21$^{-/-}$ C57Bl6 recipient mice. These mice, when transplanted with WT leukaemias, as preliminarily shown in my host lab, develop leukaemia with a latency that is comparable to that of their WT counterpart (see paragraph 5.2.4). Leukemic spleens of these mice, which consist of infiltrating WT blasts (~80-90%) and p21$^{-/-}$ TME cells, were then re-transplanted (1×10^6 cells per mouse) into WT C57Bl6 recipients. Notably, we observed significantly prolonged survival ($p < 0.001$) of these animals in comparison to a control group transplanted with WT leukaemias that had previously passaged in WT mice (Figure 6A and 6B). These data demonstrated that the absence of p21 expression in the TME, rather than in the leukemic blasts, is indispensable for activation of an immunological response against leukaemia.
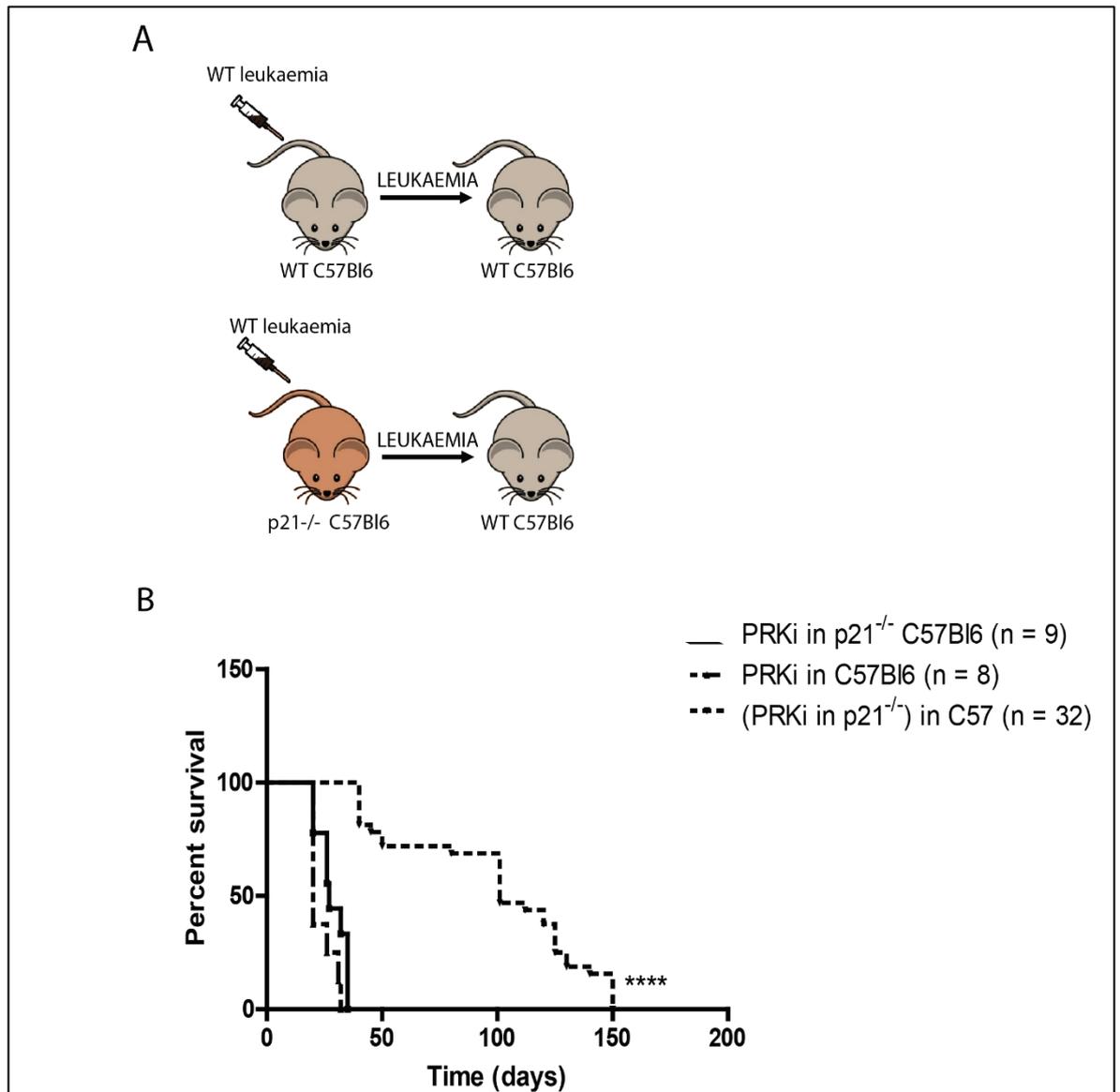
Figure 6. WT leukaemia transplantation in WT and p21$^{-/-}$ C57Bl6 mice, following re-transplantation of such leukaemias in syngeneic recipients. A) Scheme of re-transplantation. **B)** Survival curve of p21$^{-/-}$ C57Bl6 (n = 9) and WT C57Bl6 (n = 8) mice injected with WT leukaemia and survival curve of WT C57Bl6 (n = 32) mice transplanted with WT leukaemia developed in p21$^{-/-}$ C57Bl6 mice ($p < 0.001$, Gehan-Breslow-Wilcoxon test).

7.1.2 The p21$^{-/-}$ spleen and the bone marrow protect against leukaemia development

To formally prove the role of the p21$^{-/-}$ TME in mounting an anti-leukemic response, we analysed the effects of WT blasts and p21$^{-/-}$ TME separately. Due to the fact that both components are of myeloid origin, thus sharing the same myeloid-specific markers, we set them apart, by transplanting 1x10^6 WT leukaemia cells along with 5x10^6 p21$^{-/-}$ whole spleen or

bone marrow cellular extract (collected from donor p21$^{-/-}$ C57Bl6 mice) in syngeneic recipients, and monitored leukaemia growth. Leukaemias developed in mice co-transplanted with WT leukaemias and WT spleen or bone marrow cells (7 mice per group). On the contrary, leukaemia growth was completely abolished in recipients co-transplanted with WT leukaemias and either p21$^{-/-}$ spleen (7 mice) or bone marrow cells (7 mice). Strikingly, these mice remained disease-free up to 250 days post transplantation (Figure 7). These findings demonstrate that the initially observed anti-leukemic immune response activated by p21$^{-/-}$ primary leukaemias is due to the p21$^{-/-}$ TME component present in the leukemic spleens used to propagate leukaemias.
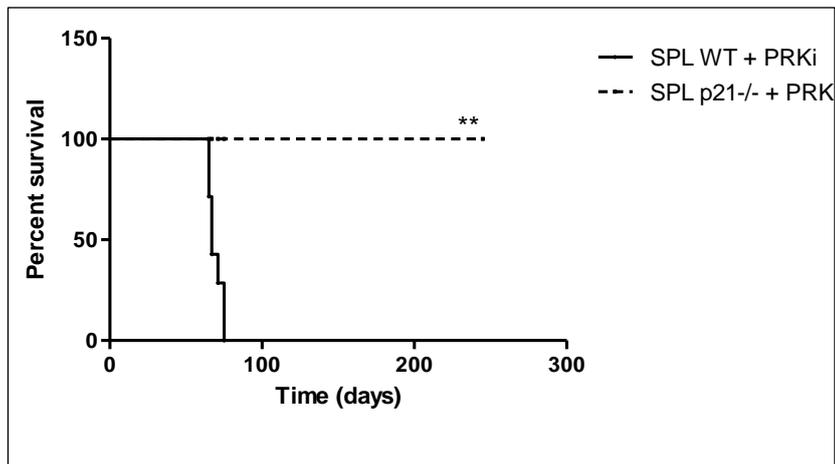
Figure 7. Survival curve of C57Bl6 syngeneic recipients transplanted with WT leukaemia along with WT or p21$^{-/-}$ spleen cells. C57Bl6 syngeneic mice transplantated with WT leukaemia along with p21$^{-/-}$ spleen cells (n=7) remained disease-free up to 250 days post iv. On the contrary, all the mice transplanted with WT leukaemia and WT spleen cells (n=7) developed the disease (p < 0.001, Gehan-Breslow-Wilcoxon test).

7.2 The p21$^{-/-}$ spleens are more sensitive to activating signals

Considering that the spleen is the anatomical site where we investigated the interactions between leukemic blasts and TME, we next analysed differences between p21$^{-/-}$ and WT C57Bl6 splenic TMEs. We first examined the activation status of the p21$^{-/-}$ and WT C57Bl6 splenic TMEs by quantifying the ratio of primary follicles and germinal centers (GC), under both steady state conditions and upon exposure to leukaemia cells. Active germinal centers

are specific sites located in the primary follicles of spleen or lymph nodes, which are characterized by the presence of proliferating mature B cells[98,99]. To detect active splenic GCs and calculate the ratio between primary follicles and GCs, we performed immunohistochemistry staining for the Ki67 proliferation marker and the Bcl6 active B-cell specific-marker. Bcl6 positivity marks the presence of B cells; Ki67 and Bcl6 stain the follicles that are immunologically active[99]. Not necessarily active GCs are double positive for Ki67 and Bcl6, since follicles at the initiation stages of their activation stain for Ki67, while they become Bcl6$^+$ only after B cells enter in the center of follicles. Although the number of active Ki67 positive GCs was similar between p21$^{-/-}$ and WT spleens at steady-state (6.7% and 6.2%, respectively; Figure 8A) , we observed slightly increased numbers of Bcl6 positive GCs in the p21$^{-/-}$ spleens, as compared to WT (6.8% and 3.7%, respectively; Figure 8B). Upon exposure to leukemic cells, active Ki67$^+$ and Bcl6$^+$ GCs increased in both WT and p21$^{-/-}$ spleens (from ~3 to 40%), yet with a faster kinetics in the p21$^{-/-}$ spleens. In fact, GCs activation peaked at 8 hours after challenge in the p21$^{-/-}$ primary follicles, while it peaked at 5 days post challenge in the WT spleen (Figure 8A and 8B). These results suggest higher sensitivity of the p21$^{-/-}$ TME to activating signals, as observed at both basal level and after tumor challenge.

A   B
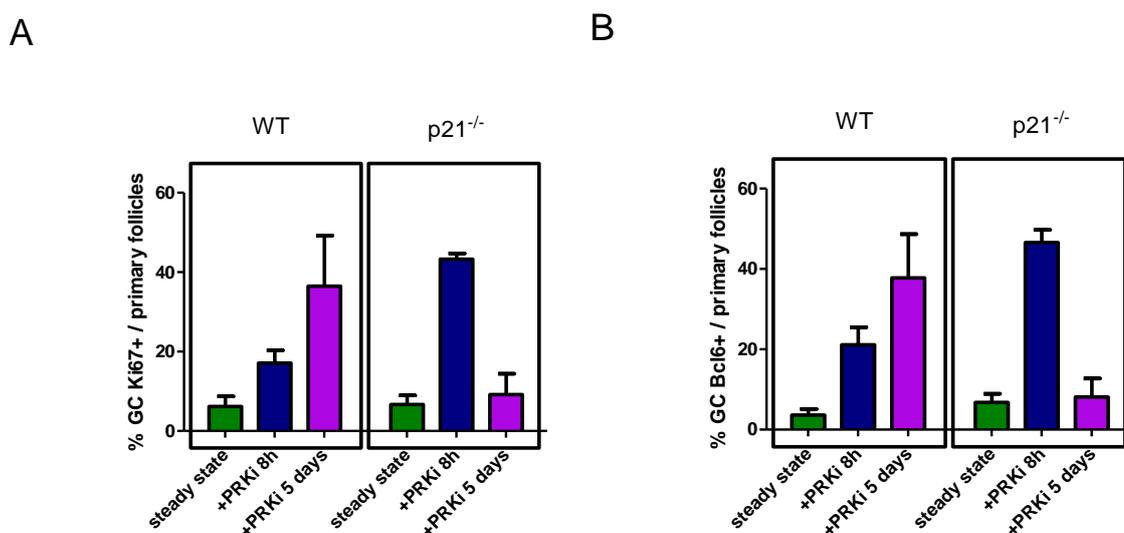
Figure 8. Response of p21$^{-/-}$ vs WT splenic TME to tumor challenge. Activation status of WT and p21$^{-/-}$ spleens represented as the ratio of **A)** Ki67$^+$ GCs and primary follicles and **B)** Bcl6$^+$ GCs and primary follicles. Values represent the

mean ± SD of two biologically independent experiments. One mouse per group was considered for each of the two biologically independent experiments.

7.3 T cells in p21$^{-/-}$ TME are not required for the early response to leukaemia exposure

The anti-leukemic immune response generated in syngeneic mice upon exposure to p21$^{-/-}$ leukemic spleens can be transferred to recipient mice by CD4$^+$ T cells (collected from syngeneic mice 15 days post leukaemia challenge) (see paragraph 5.2.2). Thus, we investigated whether T cells are recruited to the spleen already at early time points after tumor challenge. To this end, we analysed expression of CD4, CD8 and the pan-T CD3 markers within splenic primary follicles and counted positive follicles. We did not observe significant differences in the percentage of primary follicles expressing CD3, CD4 and CD8 between WT and p21$^{-/-}$ spleens, both under steady state and after leukaemia challenge (Figure 9), suggesting that T cells are not crucial for the early activation of the immune response in the p21$^{-/-}$ context. This findings imply that the observed anti-leukemic CD4$^+$ T-cell mediated response mounted by the p21$^{-/-}$ splenic TME does not occur shortly after leukaemia challenge, but later in time.
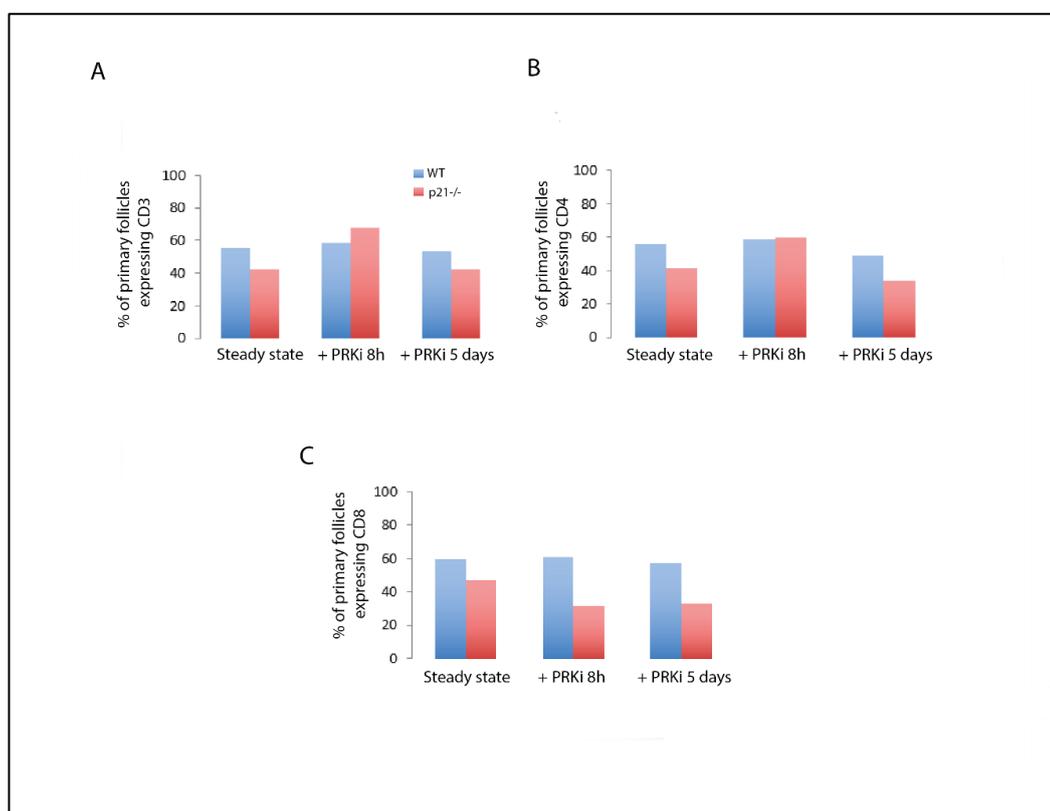
Figure 9. Analyses of T-cell compartment in p21$^{-/-}$ vs WT spleens, under steady state and upon leukaemia exposure. Percentage of primary follicles in WT and p21$^{-/-}$ spleens expressing **(A)** CD3, **(B)** CD4 and **(C)** CD8. Values represent the mean of two biologically independent experiments. One mouse per group was considered for each of the two biologically independent experiments.

7.4 Leukaemias activate p21$^{-/-}$ macrophages

7.4.1 Lack of p21 expression renders splenic macrophages more responsive to exposure to leukaemia blasts

Preliminary data of my host lab showed that the activation of a CD4$^+$ T-cell mediated response against leukaemia is MHC II-dependent (see paragraph 5.2.3). This finding, together with the observation that the p21$^{-/-}$ splenic TME is involved in the anti-leukaemia immune response (see paragraph 7.1), suggests that the key cellular mediator of the p21$^{-/-}$ TME is a professional APC. Macrophages, dendritic cells (DCs) and B-cells are all considered professional APCs. Macrophages and DCs are phagocytes that are recruited to tissues and T-cell zones of secondary lymphoid organs (lymph nodes and spleen) upon activation[100]. When activated, they constitutively express high levels of MHC II molecules and components of the antigen-processing machinery, as well as co-stimulatory molecules. Mast cells, eosinophils, and basophils (so-called atypical APCs) can also express, upon activation, MHC class II molecules on their surface, yet there is the lack of compelling evidence that they can prime naïve CD4$^+$ T cells in antigen-specific manner[100]. Thus, we mainly focused on macrophages and their function as APCs in the tumoral context.

We first examined the activation status of WT and p21$^{-/-}$ splenic macrophages under steady state conditions and upon exposure to leukemic blasts. WT and p21$^{-/-}$ C57Bl6 mice were transplanted with 5x10^6 WT leukaemia cells for tumor challenge. PRKi leukemic blasts express diverse myeloid-specific markers that overlap with those expressed on macrophages. Thus, to avoid analyses of macrophage activation in the presence of leukemic blasts in the spleen, we sacrificed the mice and collected the spleens at defined time points (8h, 24h, 48h and 7 days upon leukaemia exposure) when the blasts did not yet migrate to the splenic

environment (as determined by FACS-analysis of leukaemia blasts versus host splenocytes using the CD45.1/CD45.2 congenic model; data not shown). As a measure of macrophage response to tumor challenge, we used already established flow cytometry protocols using known markers of macrophage activation[101]. Specifically, we performed FACS analyses on the whole spleen (WT vs p21$^{-/-}$) to examine the position of CD11b$^+$ Ly6G$^-$ cells in the quadrants Ly6C and MHC II. Ly6G staining allows the exclusion of neutrophils and granulocytes, while Ly6C marks inflammatory monocytes. Differentiation of inflammatory monocytes towards macrophages is characterized by the decrease of Ly6C marker expression and in parallel, increase of MHC II expression[101]. At basal conditions, splenic p21$^{-/-}$ macrophages (defined as CD11b$^+$ Ly6G$^-$ Ly6C$^-$ MHC II$^+$) expressed increased levels of MHC II (21%; Figure 10), which characterizes an inflammatory phenotype, while WT macrophages were at their steady state (12.9%; Figure 10).

The inflammatory phenotype of p21$^{-/-}$ macrophages did not change at 8h and 24h after leukaemia exposure (17.6% and 23.2%, respectively; Figure 10), yet after 48h and 7 days post leukaemia exposure it was switched (12.6% and 3.6%, respectively; Figure 10). On the contrary, a slight increase in MHC II expression on the WT macrophages was observed only 48h post leukaemia challenge (14.8%; Figure 10), demonstrating a significantly delayed activation of WT macrophages in comparison to p21$^{-/-}$ macrophages (Figure 10). These data demonstrate a considerably faster response of already active p21$^{-/-}$ macrophages in splenic environment to tumor presence and coincide with the evidence of greater immunological responsiveness of p21$^{-/-}$ spleen to the tumor exposure (see paragraph 7.2). Moreover, it is known that also p21$^{-/-}$ macrophages in FVB strain respond with faster kinetics to tumor stimulus when compared to their WT counterpart (data obtained during the study of immunological anti-tumoral response in breast cancer; Insinga, A. *et al.* preliminary data).
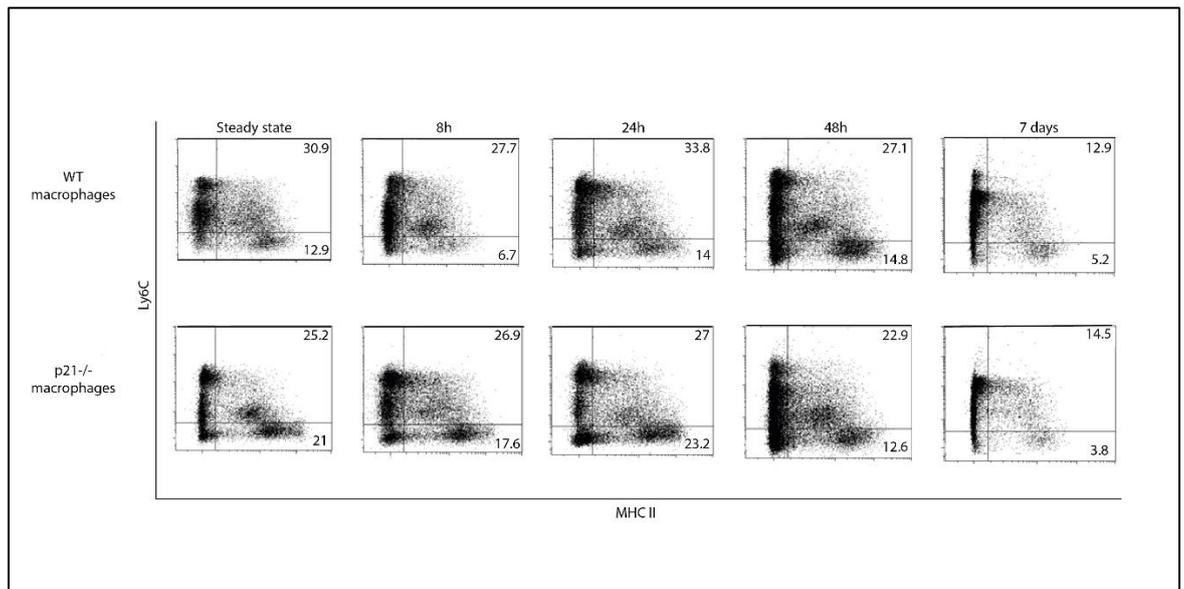
Figure 10. Kinetics of WT versus p21$^{-/-}$ splenic macrophages upon tumor stimulus. Flow cytometry plots of Ly6C/MHC II expression on CD11b$^+$Ly6G$^-$ cells in WT and p21$^{-/-}$ spleen under basal conditions and post leukaemia exposure. Data are representative of two biological replicates, using two different WT leukaemias for macrophage stimulation.

7.4.2 p21$^{-/-}$ macrophages trigger anti-tumor immune response in vivo

To examine the ability of p21$^{-/-}$ macrophages to mount the anti-tumor immune response *in vivo*, we differentiated *in vitro* macrophages from the total BM cellular extract (BM-derived macrophages; BMDMs) (see paragraph 6.5). We then transplanted 1x10^6 BMDMs (WT or p21$^{-/-}$ C57Bl6) along with WT leukaemia in syngeneic recipients. As expected, WT BMDMs failed to activate the CD4$^+$ T-cell mediated immunological response, which was followed by disease development (Figure 11). Noteworthy, 5 out of 5 mice transplanted with p21$^{-/-}$ BMDMs and WT leukaemia were disease-free up to 250 days post transplantation (Figure 11). These data clearly demonstrate that macrophages are a key cellular component of p21$^{-/-}$ TME responsible for the activation of a CD4$^+$ T-cell mediated immune response against leukaemia.
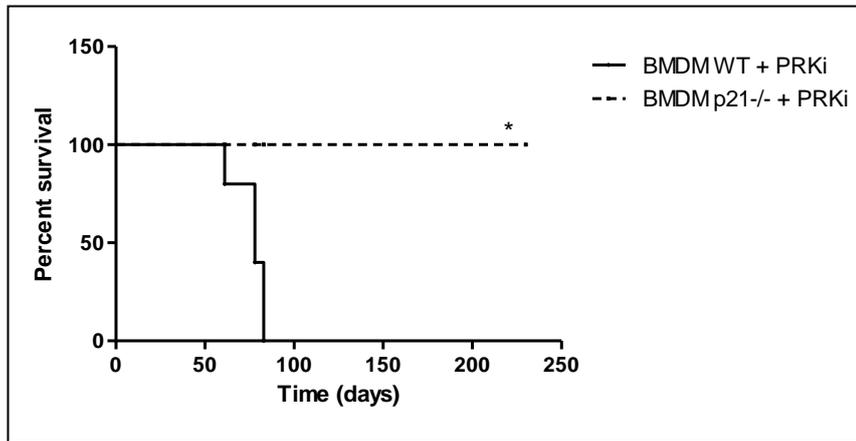
Figure 11. Survival curve of C57Bl6 syngeneic mice transplanted with WT leukaemia along with WT or p21$^{-/-}$ BMDMs. C57Bl6 mice transplanted with WT leukaemia and WT BMDMs (n = 5) developed the disease while the recipients injected with WT leukaemia and p21$^{-/-}$ BMDMs (n = 5) remained disease-free ($p < 0.05$, Gehan-Breslow-Wilcoxon test).

7.5 The macrophage response to non-tumoral stimuli is p21-independent

7.5.1 Bone marrow-derived macrophages respond to unspecific stimuli in a p21-independent manner

To further characterize functional differences between p21$^{-/-}$ and WT C57Bl6 macrophages, we analysed canonical activation signatures upon *in vitro* priming of BMDMs and stimulation with IFN-γ and LPS. BMDMs were incubated with IFN-γ for 6 hours and then treated with LPS. 24 hours post LPS stimulation, we performed FACS analysis for known markers of macrophage activation, as previously described (see paragraph 7.4.1). WT and p21$^{-/-}$ BMDMs (CD11b$^+$ Ly6G$^-$ Ly6C$^-$) expressed modest level of MHC II under basal conditions (9.4% and 5.9%, respectively). Following priming and stimulation with IFN-γ and LPS, both WT and p21$^{-/-}$ BMDMs showed similar activated phenotype: increased expression of MHC class II antigens (88.7% and 80%), demonstrating that p21$^{-/-}$ and WT BMDMs share a comparable activation signature upon canonical stimulation. Thus, the p21$^{-/-}$ macrophage responsiveness seems to be specific for the tumoral stimulus.

7.5.2 Splenic macrophages are resistant to chronic and acute DNA damage

p21 is involved in the cellular response to DNA-damage and is critical for DNA-repair, as revealed by findings of DNA-damage accumulation in cells lacking p21 expression[4]. Thus, we hypothesised that splenic macrophages from p21$^{-/-}$ mice have chronic activation of DNA-repair signalling pathways and accumulate excessive DNA damage, which may interfere with their immune functions. We first investigated whether WT splenic macrophages mimic the phenotype of p21$^{-/-}$ macrophages upon induction of DNA damage. To induce chronic DNA damage, we treated WT C57Bl6 mice with N-ethyl-N-nitrosourea (ENU), a potent DNA-damaging agent[16]. A single dose of ENU was administered intraperitoneally (50mg/kg), and mice were sacrificed 5 and 10 days post treatment. Spleens were collected, stained with antibodies against CD11b and the γ-H2AX DNA-damage marker, and analysed by immunofluorescence. Intensity and number of γ-H2AX$^+$ foci represent informative parameters to measure DNA damage. Surprisingly, p21$^{-/-}$ CD11b$^+$ cells did not show DNA damage accumulation under steady state conditions, as compared to WT counterparts (Figure 12). Upon ENU administration, we observed a slight γ-H2AX signal accumulation in WT or p21$^-$CD11b$^-$ cells at 5 or 10 days post treatment. Strikingly, levels of γ-H2AX expression in CD11b$^+$ cells, instead, did not increase after ENU treatment, and were indeed comparable to those of the untreated cells (see Figure 13 for representative results on WT cells). These results demonstrate that, unexpectedly, splenic macrophages are not susceptible to accumulation of chronic DNA damage or, alternatively, they have a different processing of the DNA damage.
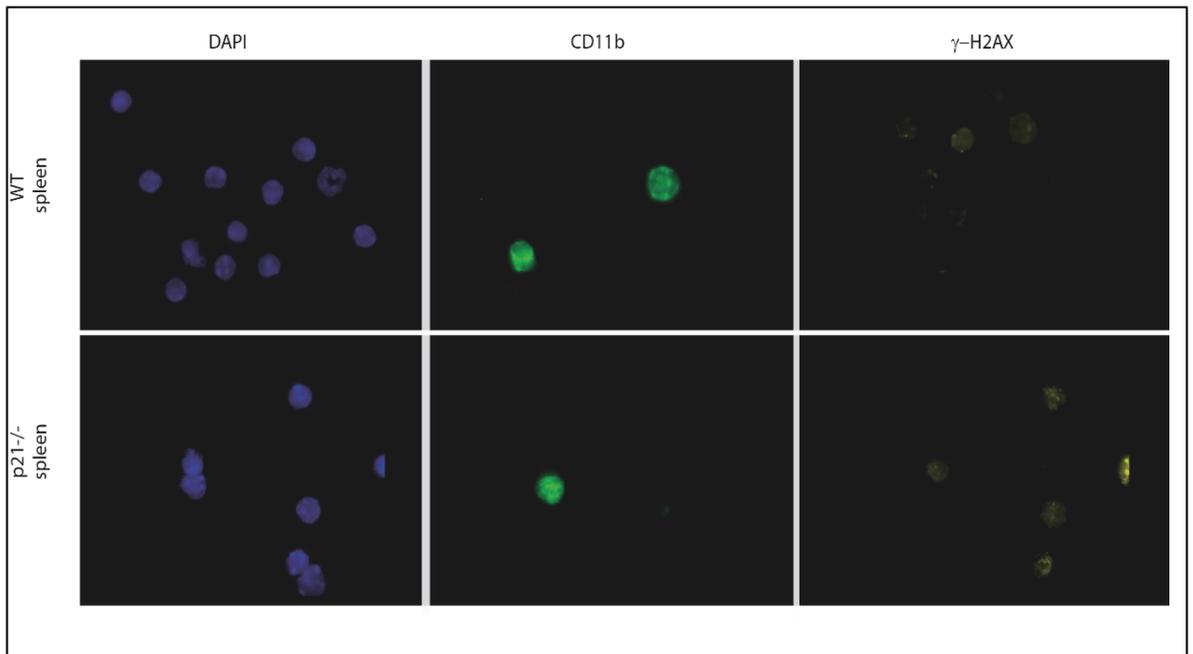
Figure 12. DNA damage in p21$^{-/-}$ vs WT splenic macrophages. Immuno-fluorescence analysis of DAPI (blue, x40), CD11b (green, x40) and γ-H2AX (yellow, x40) on WT and p21$^{-/-}$ spleens. Images shown are representative of three biological replicates.
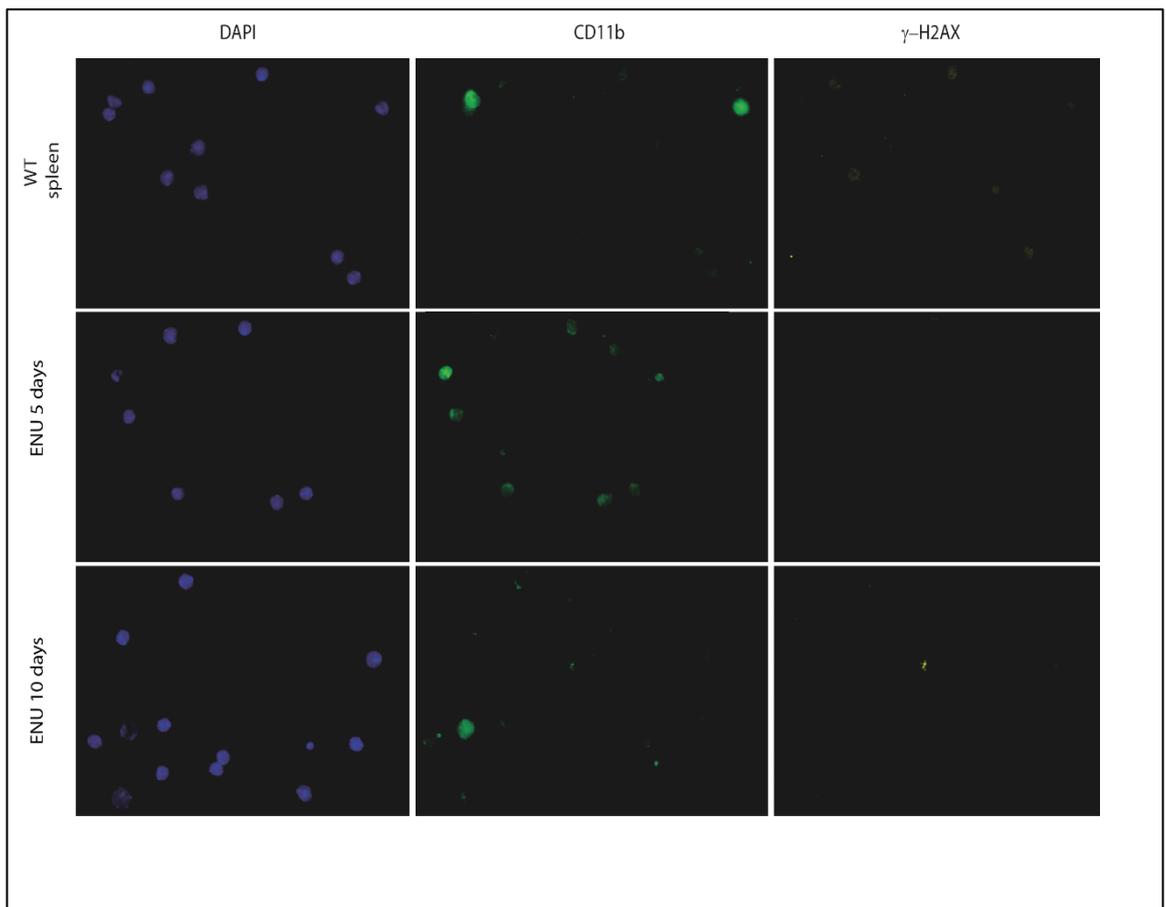
Figure 13. ENU-induced DNA damage in WT macrophages. Immunofluorescence analysis of γ-H2AX expression in WT CD11b$^+$ and CD11b$^-$ splenocytes upon 5 or 10 days ENU treatment (DAPI: blue; CD11b: green; γ-H2AX: yellow; x40). Data shown are representative of three biological replicates.

We then used γ-irradiation as a source of acute DNA damage and assessed levels of DNA damage in CD11b$^+$ splenic macrophages of WT C57Bl6 mice. We irradiated mice using different sub-lethal doses of γ-irradiation (2, 4 and 6 Gy). Mice were sacrificed immediately after γ-irradiation and spleens were collected and processed for immunofluorescence analysis of γ-H2AX foci formation. While cells negative for CD11b expression were clearly damaged upon γ-irradiation, macrophages were resistant to DNA damage accumulation (Figure 14). These data, together with the observed resistance to chronic DNA damage, indicate that splenic macrophages, independently of p21 expression levels, have unique mechanisms of DNA damage processing.
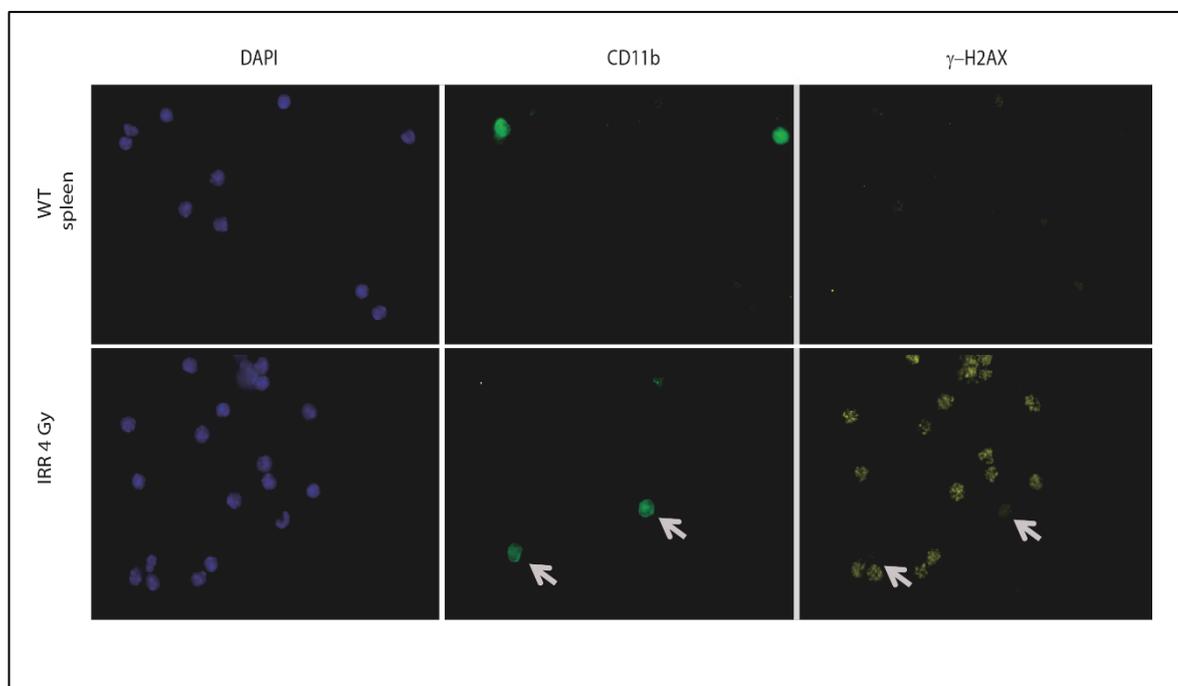
Figure 14. Irradiation-induced DNA damage in WT macrophages. Immunofluorescent staining of spleens collected from WT mice previously irradiated 4 Gy (DAPI: blue; CD11b: green; γ-H2AX: yellow; x40). While γ-H2AX signal is present in CD11b$^-$ cells, macrophages do not accumulate DNA damage upon irradiation, as indicated with white arrows. Presented images are of 4 Gy irradiated spleens, since 2 Gy and 6 Gy irradiation induces the same level of DNA damage (not shown). Images are representative of two biological replicates.

7.6 Conventional p21$^{-/-}$ macrophage subpopulations are not involved in the anti-leuke-mic immune response

7.6.1 CD11b or CD11c markers do not allow identification of the p21$^{-/-}$ APC involved in the anti-leukemic immune response

To isolate and characterize the specific p21$^{-/-}$ APC responsible for the anti-leukaemia immune response, we tested the ability of diverse p21$^{-/-}$ APCs to trigger an immunological response against WT leukaemia in immune-competent hosts. CD11b$^+$ (a marker mainly expressed by macrophages) and CD11c$^+$ (a marker mainly expressed by DCs) cells were isolated via magnetic separation from spleens of WT and p21$^{-/-}$ C57Bl6 mice. We transplanted $1x10^6$ of WT or p21$^{-/-}$ CD11b$^+$ or CD11c$^+$ cells along with $1x10^6$ WT leukaemia cells in syngeneic recipients. The protective immunological response against the disease was not activated neither in presence of p21$^{-/-}$ CD11b$^+$ nor CD11c$^+$ cells, since all the experimental groups developed leukaemia with comparable latency to their WT counterpart (span of 35-40 days; data not shown). These results show that expression of CD11b or CD11c markers alone does not allow identification of the relevant p21$^{-/-}$ APC. Indeed, diverse APCs can share same superficial markers and specific combination of markers characterize discrete subpopulations of APCs.

7.6.2 Other conventional macrophage markers do not allow identification of the p21$^{-/-}$ APC involved in the anti-leukemic immune response (F4/80, CD68, CD169, CD206, Dectin-2, CD209b, Marco, Iba1)

Data described above suggest that cellular mediators of the anti-leukemic immune response in the p21$^{-/-}$ TME are discrete subpopulations of APCs. We thus considered the usage of a combination of additional cellular markers and of different methodologies of identification.

The distinction of tissue macrophage subpopulations can be achieved by their ontogeny. While some can be of a mixed origin, most of splenic macrophages are either derived from embryonic precursors or monocytes, yet their diverse origin-dependent functions are still not

fully clear[102]. Moreover, in the spleen, different subpopulations of macrophages (such as metallophilic, marginal zone, red and white pulp macrophages) are phenotypically distinguishable and can be found in discrete niches of the tissue were they possess specific immunological functions[103].

To identify the specific subpopulation of p21$^{-/-}$ macrophages that act as potent mediator of immunological response against tumor, we examined splenic macrophage subpopulations of different origin, by flow-cytometry analyses of known markers of embryonic- (CD11b$^+$F4/80$^{low/neg}$) and monocyte-derived macrophages (F4/80$^+$). The percentage of either embryonic- or monocyte-derived macrophages was low (1.2% and 2.05%, respectively), without significant differences between spleens collected from healthy WT or p21$^{-/-}$ C57Bl6 mice.

We then analysed metallophilic (CD68$^+$CD169$^+$), red pulp (CD68$^+$F4/80$^+$CD206$^+$Dectin-2$^+$) and marginal zone (CD68$^+$CD209b$^+$Dectin-2$^+$Marco$^+$) macrophage subpopulations. Flow-cytometry analyses were performed on spleens collected from mice under steady state conditions and upon previous exposure to WT leukaemia blasts. WT leukemic blasts, like all the above-mentioned macrophage subpopulations, express the CD68 marker (48.7% ± 3.3). Therefore, to avoid presence of the CD68$^+$ blasts in the spleen, we analysed spleens collected before the infiltration of the organ by leukemic blasts (8 hours and 5 days post leukaemia challenge). Macrophage subpopulations were present in a very low amount both in the p21$^{-/-}$ and WT spleens, independently of leukaemia exposure (Table 3). Data shown here imply that the usage of conventional markers of diverse macrophage subpopulations is not sufficient for identification of key p21$^{-/-}$ APC that triggers anti-tumoral response.

	% Metallophilic macropages	% Red pulp macropages	% Marginal zone macropages
WT	0.8 ± 0.1	0.8 ± 0.2	0.6 ± 0.3
p21-/-	1.3 ± 0.3	1.1 ± 0.1	0.5 ± 0.1
WT + PRKi 8h	0.2	0.5	0.01
p21-/- + PRKi 8h	0.2	0.2	0.03
WT + PRKi 5 days	0.2	0.4	0.01
p21-/- + PRKi 5 days	0.4	0.4	0.02

Table 3. Metallophilic, red pulp and marginal zone macrophages in WT and p21^{-/-} spleen. Flow-cytometry analysis of CD68^{+}CD169^{+} (metallophilic), F4/80^{+}CD206^{+}Dectin-2^{+} (red pulp) and CD68^{+}CD209b^{+}Dectin-2^{+}Marco^{+} (marginal zone). Numbers of macrophage subpopulations under steady state are represented as the average value of three individual experiments ±SD. The analyses on spleen challenged with leukaemia were performed once.

As additional approach to examine physical distribution of macrophages in WT and p21^{-/-} spleens (both under steady state and upon leukaemia exposure), we performed immunohisto-chemistry analysis of specific macrophage markers. The detection of macrophages was assessed using the well-characterized "Pan-macrophage" marker Iba1 (Ionized calcium-binding adapter molecule 1). Iba1 is a 17-kDa protein that is constitutively expressed on macrophages and microglia[104]. We observed a diffuse signal of Iba1 and equal expression of the protein in all of the samples tested (Figure 15). The constitutive expression of Iba1 in splenic macrophages, independently on their p21 status, excludes its usage for the appreciation of differences among spleen samples in our conditions.
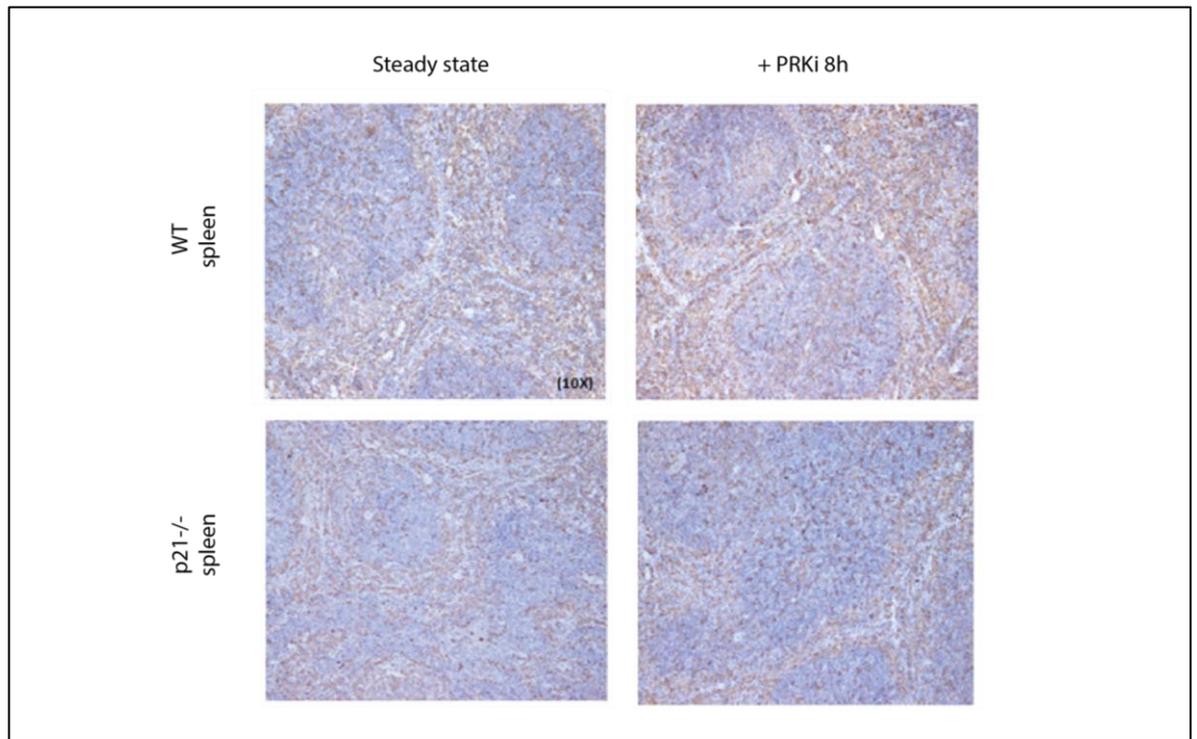
Figure 15. Iba1 expression in WT and p21$^{-/-}$ spleens. Anti-Iba1 immuno-staining performed on WT and p21$^{-/-}$ spleens, both under steady state and post leukaemia exposure (brown staining indicates Iba1 positive cells). Images are representative of two biological replicates. One mouse per group was considered for each of the two biological replicates.

CD68 or macrosialin is a member of scavenger receptor supergene family. It is a known Pan-macrophage marker mainly expressed in their late endosomes and lysosomes. In comparison to Iba1, this is a more selective marker, since it is expressed predominantly on activated macrophages[105]. We analysed the expression of CD68 protein in WT and p21$^{-/-}$ spleens, both under steady state and upon exposure to leukaemia. Comparing the slides of p21$^{-/-}$ vs WT spleens, we noticed a higher level of CD68 positivity in p21$^{-/-}$ spleens under steady state compared to its WT counterpart (Figure 16). Moreover, we observed the increase in CD68 expression after challenge with leukaemia mainly in p21$^{-/-}$ spleen (Figure 16), suggesting that upon tumor challenge, a different recruitment of macrophages occurs in the p21$^{-/-}$ splenic TME, as compared to its WT counterpart (these observations are based on visual analyses of the samples; the quantification of CD68^{+} cells in the samples has not been performed since this analysis served as an informative step preceding further analyses).
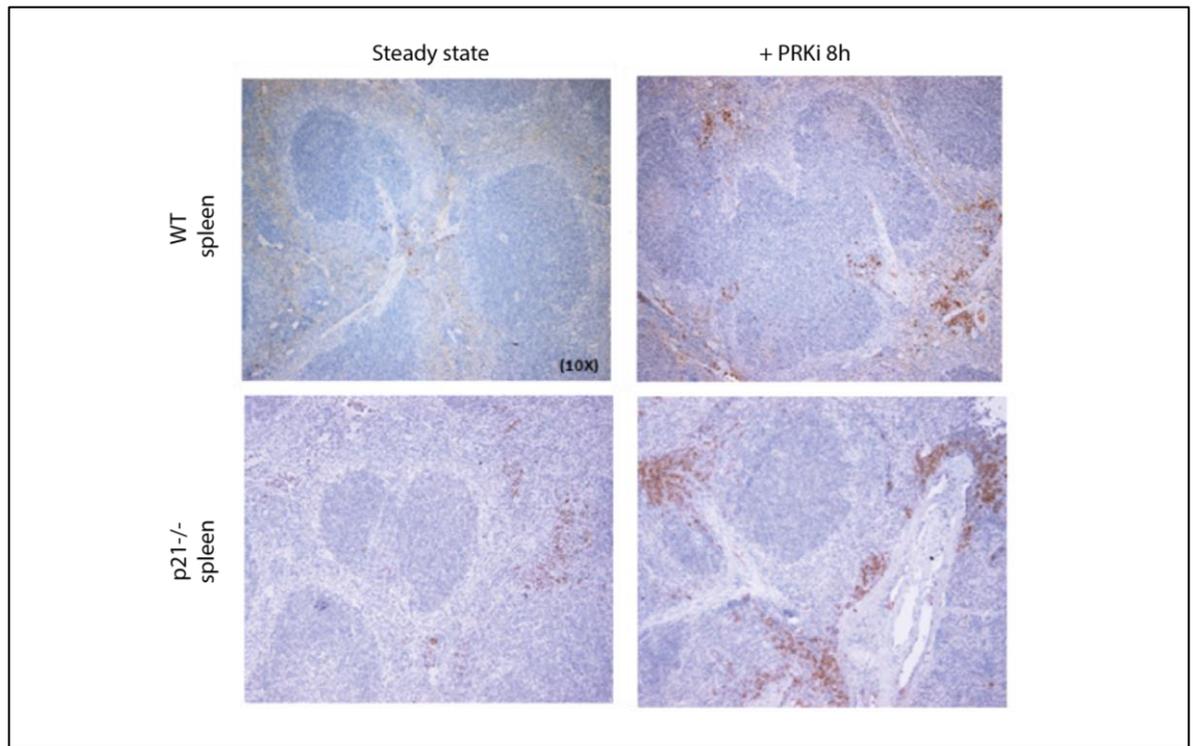
Figure 16. CD68 expression in p21^{-/-} vs WT spleens. Anti-CD68 immunostaining (brown staining indicates CD68 positive cells) of p21^{-/-} and WT spleens under steady state and 8h post leukaemia exposure. Images are representative of two biological replicates. One mouse per group was considered for each of the two biological replicates.

7.7 Identification of Fe-loaded CD68^{+} macrophages (iTAMs) as potential effectors of the immune-response against leukaemia cells

7.7.1 Exposure to leukaemia blasts induces iron-retention in splenic macrophages

Apart from their contribution to immunity, splenic macrophages have a crucial role in recycling iron from senescent red blood cells[68]. Thus, we analysed the presence of iron-containing macrophages in WT and p21^{-/-} spleens, by Perls' staining, which marks iron (Fe) particles in the tissue. As expected, at steady state, Fe particles were detected mainly in the red pulp in both p21^{-/-} and WT splenic macrophages (Figure 17). Upon leukaemia exposure, the signal of Fe increased both in p21^{-/-} and WT macrophages, suggesting that the challenge with leukaemia cells induced Fe-retention in macrophages (Figure 17). Interestingly, we observed a difference in the physical position of p21^{-/-} and WT Fe-loaded macrophages upon tumor challenge. While the WT Fe-loaded macrophages remained detectable in the red pulp, p21^{-/-} Fe-loaded macrophages were found also inside primary follicles (Figure 17), suggesting

different functional characteristics of Fe-loaded p21$^{-/-}$ splenic macrophages in the presence of leukaemia blasts.
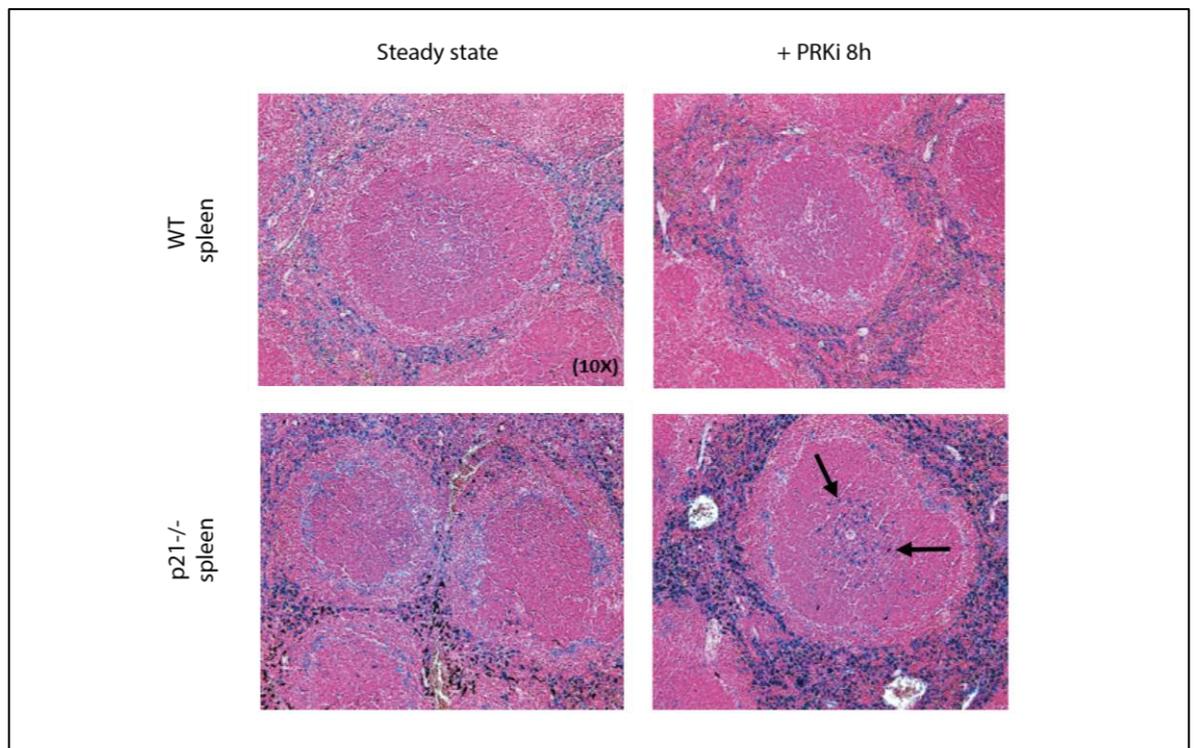
Figure 17. Iron content in p21$^{-/-}$ vs WT splenic macrophages. Perls' staining of WT and p21$^{-/-}$ spleens, both under steady state and post exposure to leukaemia. Blue colour indicates intracellular iron. p21$^{-/-}$ Fe-loaded macrophages inside primary follicles of p21$^{-/-}$ spleens are indicated with black arrows. Images are representative areas of two biologically independent samples. One mouse per group was considered for each of the two biological replicates.

7.7.2 Exposure to leukaemia blasts induces accumulation of Fe-loaded CD68$^+$ macrophages (iTAMs) only in p21$^{-/-}$ spleens

To phenotypically characterize the p21$^{-/-}$ Fe-loaded macrophage subpopulation present in primary follicles of p21$^{-/-}$ spleen upon leukaemia exposure, we performed stainings with Perls' and anti-CD68 antibodies on consecutive sections of the paraffinized spleen tissue. We identified an Fe-loaded macrophage subpopulation that also expresses CD68 and, strikingly, is present only in the p21$^{-/-}$ spleen (Figure 18). The Fe-loaded CD68$^+$ macrophages, named iTAMs, have been identified in TME of NSCLC, where they exhibit anti-tumoral function (see paragraph 5.5.1.3).

Notably, we observed the presence of iTAMs also in p21$^{-/-}$ lung cancers. We analysed WT and p21$^{-/-}$ K-Ras/RERT lung cancer[106]. We performed CD68 immunostaining on the slides of WT and p21$^{-/-}$ lung cancer which were previously stained with Perls' and documented the presence of the Fe-loaded macrophages exclusively in the p21$^{-/-}$ TME, mainly in tumor-free areas of lung sections (Figure 19A). Strikingly, some of the p21$^{-/-}$ Fe-loaded macrophages were also positive for CD68 staining (iTAMs) (Figure 19B).

Together, these data establish a correlation between tumor cells and the presence of p21$^{-/-}$ iTAMs in the TME, in both leukaemias and lung cancer, and suggest that the presence of p21$^{-/-}$ iTAMs in the TME is linked with the anti-tumoral immune response activated by the p21$^{-/-}$ TME.
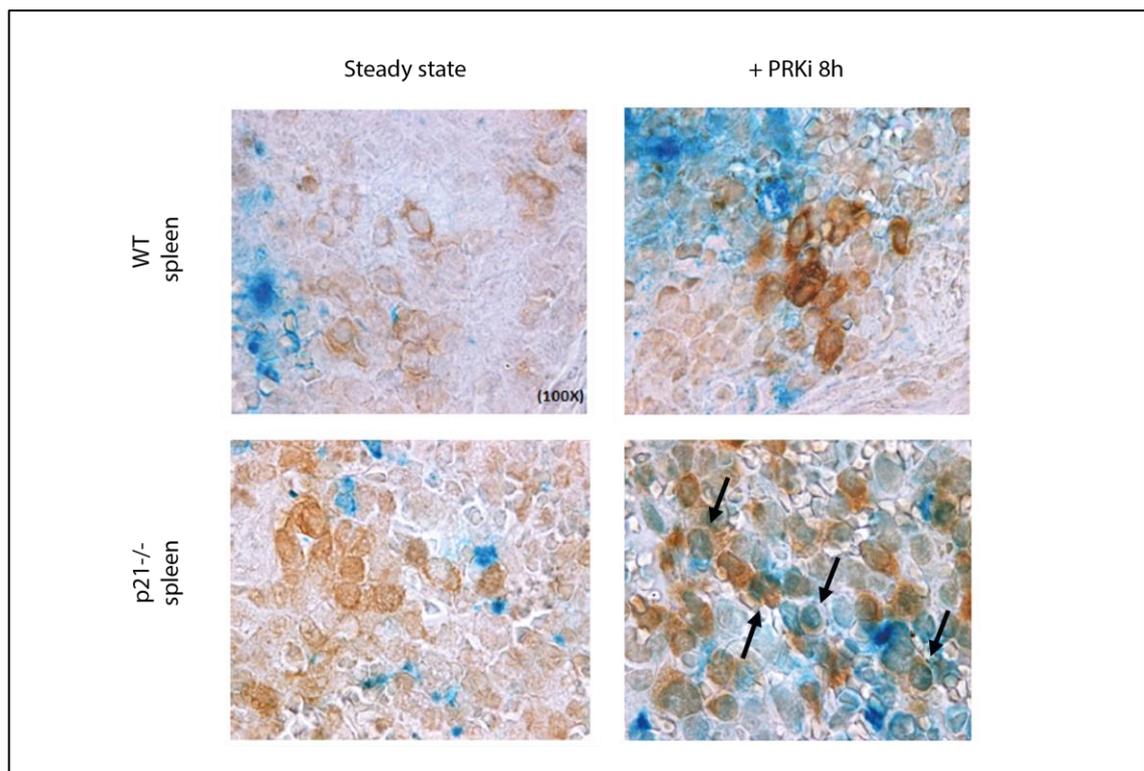
Figure 18. p21$^{-/-}$ Fe-loaded macrophages express CD68. Overlapping Perls' staining and anti-CD68 immunostaining of WT and p21$^{-/-}$ spleens under basal conditions and upon tumor challenge. Blue staining indicates iron and brown staining indicates CD68 positive cells. Black arrows indicate p21$^{-/-}$ CD68^{+} iron-loaded macrophages. Images are of the areas representative of two biological replicates. One mouse per group was considered for each of the two biological replicates.
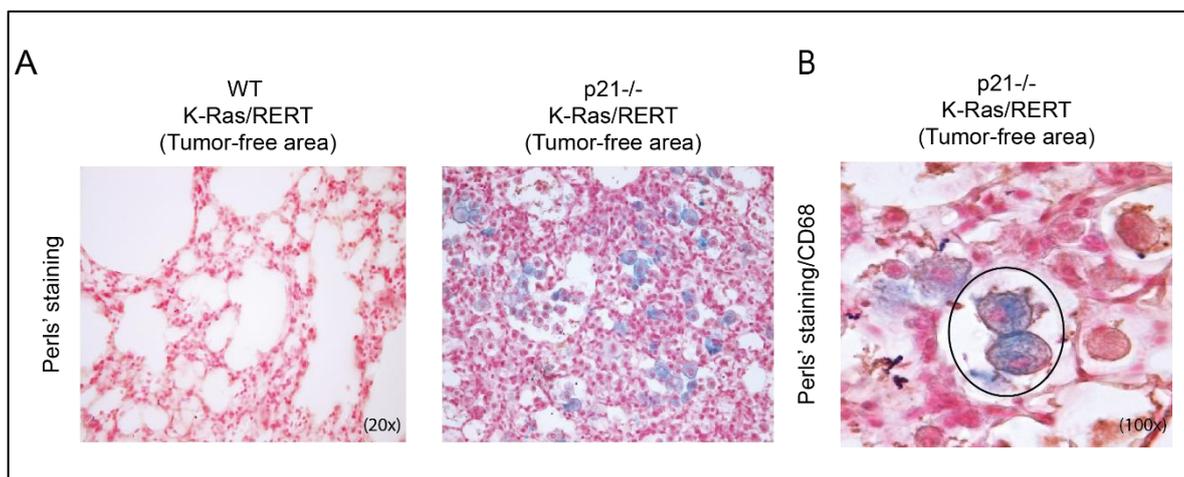
Figure 19. CD68 immune-staining and Perl's staining of non-tumoral areas of WT vs p21^{-/-} K-Ras/RERT Lung carcinoma. A) Perls' staining of tumor-free areas of WT and p21^{-/-} K-Ras/RERT lung cancer (blue staining indicates iron). **B)** Overlapped staining for CD68 and Perl's on tumor-free area of p21^{-/-} K-Ras/RERT lung cancer (brown staining indicates CD68 positive cells and blue indicates Fe-loaded cells). Images are of the areas representative of two biological replicates. One mouse per group was considered for each of the two biological replicates.

7.8 Polarization of splenic macrophages is marginally affected by modulation of systemic iron content

7.8.1 Systemic iron depletion induces a mild shift in macrophage polarization in p21-null context

Macrophages are key regulators of iron homeostasis, and their polarization is known to dictate expression of genes involved in iron metabolism, or vice versa[67]. Modulating iron content in macrophages can result in a shift of macrophage polarization.

We examined the polarization of WT and p21^{-/-} splenic macrophages upon systemic iron depletion, using a known iron chelator desferoxamine (DFO)[107]. 100mg/kg DFO were injected intraperitoneally in WT and p21^{-/-} C57Bl6 mice and, 15h post treatment, mice were sacrificed and spleens collected. We FACS-sorted CD11b^{+}F4/80^{+} macrophages and performed qPCR analysis for diverse macrophage polarization markers (tumor necrosis factor alpha (TNFα), transferrin receptor 1 (Tfr1), hypoxia inducible factor alpha (Hif1α), iron-regulated transporter 1 (Ireg1), heme oxygenase 1 (HO1)). Analyses of mRNA expression of the above-mentioned macrophage markers did not show differences between WT and p21^{-/-} splenic macrophages under steady state conditions (data not shown). By comparing fold-

changes of DFO-treated versus untreated samples obtained by p21$^{-/-}$ splenic macrophages to the ones of their WT counterpart, we observed a drop in transferrin receptor 1 and the Fe-exporter Ireg1 (data not shown). These data would suggest a different handling of Fe-intake in p21$^{-/-}$macrophages in response to exogenous iron depletion. These results, together with the lack of induction of HO1, suggest a mild shift towards M1-like phenotype[69] of p21$^{-/-}$ macrophages, as compared to WT; however the expression of only few of the iron-related markers seems to change upon DFO treatment (Ireg1 upregulation and Trf1 downregulation).

7.8.2 Macrophages are not responsive to systemic iron-overload

In parallel, we studied WT and p21$^{-/-}$ splenic macrophage polarization after treatment with hemin, which is known to induce iron-overload[97]. A single dose of hemin (75uM/kg) was intravenously injected in WT and p21$^{-/-}$ C57Bl6 mice, and, after 15h mice were sacrificed. We FACS-sorted CD11b$^+$F4/80$^+$ macrophages from spleens of these mice, and examined expression of M1/M2 related genes (see paragraph 7.8.1). Fold-change levels (treated versus untreated samples) for the p21$^{-/-}$ splenic macrophages and their WT counterpart showed that systemic iron overload did not affect polarization of WT or p21$^{-/-}$ macrophages (data not shown).

7.9 Experienced challenges with p21$^{-/-}$ mouse strain

In 2017 it became progressively evident that some of the initial observations described in the above chapters were not reproducible. In particular: a) transplantation of p21$^{-/-}$ splenocytes in WT mice failed to protect against growth of WT leukaemias (34 mice); b) faster kintetics of p21$^{-/-}$ splenic macrophage response to leukaemia challenge were not reproduci-

ble in two independent experiments; c) co-transplantation of p21^{-/-} BMDMs with WT leukaemia failed to promote anti-tumoral immune response in 14 mice (p21^{-/-} BMDMs were produced from p21^{-/-} BM cells, collected from 5 p21^{-/-} C57Bl6 mice separately).

Considering the robustness of the previously observed phenotypes, we hypothesized that lack of reproducibility was connected to a modification of the status of the p21^{-/-} C57Bl6 mouse colony. Notably, during the 2016-2017 years, we also noticed a gross modification of the tumor-phenotype of the p21^{-/-} PML-RAR expressing (PRKi) mice, which did not develop leukaemias during their entire lifespan, as instead consistently observed in previous years (see also ref. 16).

For unknown reasons, in the course of 2018, resistance of p21^{-/-} PRKi mice "disappeared", and several mice developed leukaemias, which, most notably, were unable to transplant in immune-competent syngeneic mice, as previously observed. Importantly, these leukaemias were also capable of generating protective T cells (as shown by adoptive T-cell transfer of CD4^{+} T cells obtained from WT mice challenged with p21^{-/-} leukaemias). We were unable, however, to reproduce experimentally the ability of the p21^{-/-} TME (spleen, bone marrow or macrophages) to protect WT mice toward the growth of WT leukaemias.

In summary, during the 2016-2018 years, we observed: i) initially, the non-reproducibility of the main traits of the previously observed p21^{-/-} phenotype (occurrence of leukaemias in the p21^{-/-} background; capacity of the p21^{-/-} TME to induce resistance to leukaemia growth in WT mice); and ii) more recently, the partial re-appearance of some traits of the p21^{-/-} phenotype (development of leukaemias in the p21^{-/-} PRKi mice; lack of their transplantability in syngeneic WT mice; capacity to mount a protective T-cell response), but not others (capacity of the p21^{-/-} TME to transfer resistance to leukaemia growth).

To explain these findings, we hypothesized that the p21^{-/-} colonies (p21^{-/-} and p21^{-/-} PRKi) might have segregated specific genetic loci with immune-related functions. To test this hypothesis, we started a new p21^{-/-} colony by crossing C57 WT and C57 p21^{-/-} mice (using

either "our" mice or new mice imported from Jaxon Laboratories), and then breeding heterozygous mice to re-generate "new" homozygous p21$^{-/-}$ mice. However, the p21$^{-/-}$ TME from mice of these two new colonies proved to be unable to protect against leukaemia development.

As an alternative hypothesis, we are now considering the existence of environmental factors (possibly due to our mouse-housing conditions) that may affect the immunological status of the p21$^{-/-}$ mice. Unfortunately, however, we could not identify changes in our mouse-housing conditions that could be tested experimentally. Thus, we are now evaluating the possibility of analysing the microbiota of p21$^{-/-}$ mice of different strains (C57Bl6 vs FVB; see below) and eventually test their impact on the immunity of our mice.

Meanwhile, we decided to investigate the previously observed p21$^{-/-}$ phenotype in another mouse strain (FVB).

7.10 The p21$^{-/-}$ TME is critical to leukaemia development and growth in the FVB mouse strain

7.10.1 p21$^{-/-}$ FVB mice are resistant to leukaemia formation

It has been demonstrated in the host lab that the p21-dependent CD4$^+$ T-cell mediated immunological response against tumor also occurs in breast cancer (see paragraph 5.2.5). Notably, the mouse model of breast cancer (WT and p21$^{-/-}$) used in these studies (FVB strain) is of a different genetic background than the one used in leukaemia studies (C57Bl6 strain), suggesting that the potent immune response observed with leukaemias is neither strain nor tumor-type specific. Thus, we investigated whether in the absence of p21, TME of different genetic backgrounds possesses similar tumor-clearance functions. We first generated and then tested an AML in the FVB WT and p21$^{-/-}$ mouse strains. To this end, WT and p21$^{-/-}$ Lin$^-$ cells (obtained from FVB and p21$^{-/-}$ FVB, respectively) were transduced with a retrovirus

expressing the AML-specific MLL-AF9 fusion-protein oncogene and transplanted into WT and p21$^{-/-}$ FVB recipient mice. Most notably, p21$^{-/-}$ Lin$^-$ cells expressing MLL-AF9 failed to promote leukaemogenesis when expressed in either WT or p21$^{-/-}$ mice (data not shown). WT Lin$^-$ cells expressing MLL-AF9 engrafted and induced leukaemia in WT recipients, but not in p21$^{-/-}$ mice (Figure 20). Engraftment was not observed in p21$^{-/-}$ recipients, and they remained disease-free (Figure 20). These results suggest that p21 expression is critical for the permissiveness of FVB mice to leukaemia formation.
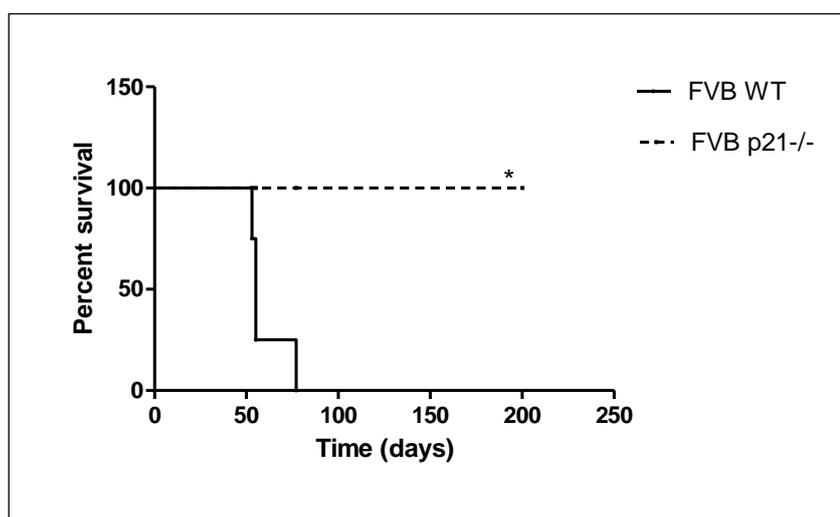
Figure 20. Survival curve of WT vs p21$^{-/-}$ FVB mice transplanted with WT Lin$^-$ cells expressing MLL-AF9. WT FVB mice (n = 4) all developed leukaemia, while p21$^{-/-}$ recipients (n = 4) remained disease-free ($p < 0.05$, Gehan-Breslow-Wilcoxon test).

7.10.2 The p21$^{-/-}$ FVB TME is not permissive for leukaemia growth

To investigate whether the p21$^{-/-}$ TME of FVB mice has also an impact on the growth of already formed leukaemias, we transplanted 1×10^6 cells from a fully developed WT MLL-AF9 leukaemias (previously generated in WT recipients, by injection WT Lin$^-$ cells infected with MLL-AF9) in both WT and p21$^{-/-}$ mice. As expected, leukaemias propagated in WT recipients, while leukaemia growth was halted in 4 out of 4 p21$^{-/-}$ recipients (Figure 21). These data parallel those obtained with breast cancer in p21$^{-/-}$ FVB recipients, and demonstrate the ability of p21$^{-/-}$ FVB TME components to mount an immunological response against different types of tumors.
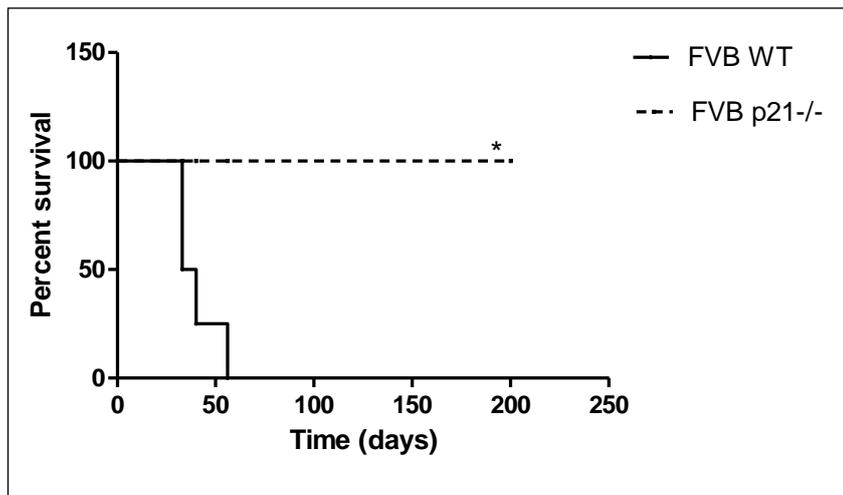
Figure 21. Survival curve of WT vs p21$^{-/-}$ FVB mice transplanted with WT MLL-AF9 leukaemia. WT FVB recipients all developed leukaemia (n = 4), while p21$^{-/-}$ FVB mice (n = 4) remained disease-free up to 200 days post injection ($p <$ 0.005, Gehan-Breslow-Wilcoxon test).

Experiments to characterize the role of macrophages in anti-leukaemia immune response activation in FVB context are ongoing.

7.11 Human cord blood CD34$^+$ cells give rise to human immune system in NOD-scidIL2Rgammanull mouse model

7.11.1 Generation of humanized mouse model

In order to investigate whether the anti-tumoral T-cell mediated immune response triggered by p21$^{-/-}$ iTAMs could occur in humans, we generated a humanized mouse model. One of the best established approaches to humanize NSG mice is transplanting human CD34$^+$ cells,

that include haematopoietic stem and progenitor cells, which are able to give rise to the human immune system in mouse recipients. Thus, we transplanted human CD34$^+$ cells from the cord blood of healthy donors (hCB-CD34$^+$) into sub-lethally (1 Gy) irradiated NOD-*scid*IL2Rgamma^{null} (NSG) mice (Figure 22A). The engraftment of hCB-CD34$^+$ was followed in peripheral blood (PB) via FACS analysis using human CD45 marker. 7 weeks post transplantation, the percentage of hCD45$^+$ cells in PB of transplanted mice was higher than 20% and mice were considered humanized (Figure 22A).

7.11.2 In vivo propagation of hCB-CD34$^+$ cells

In order to amplify hCB-CD34$^+$ cells and propagate hCB-CD34$^+$ humanized NSG mice, the whole BM of hCB-CD34$^+$ NSG mice was intravenously injected into irradiated NSG recipients (Figure 22B). The engraftment of hCB-CD34$^+$ cells was detected already 6 weeks post transplantation (Figure 22B), which could be due to stimulated self-renewal capability of hCB-CD34$^+$ cells upon re-transplantation. On the other hand, NSG mice transplanted with BM of second passage hCB-CD34$^+$ NSG mice did not show any sign of engraftment even 16 weeks post injection (Figure 22C). Taken together these observations might be explained by the fact that hCB-CD34$^+$ cells are pushed to proliferate and rapidly undergo functional exhaustion in this model system.
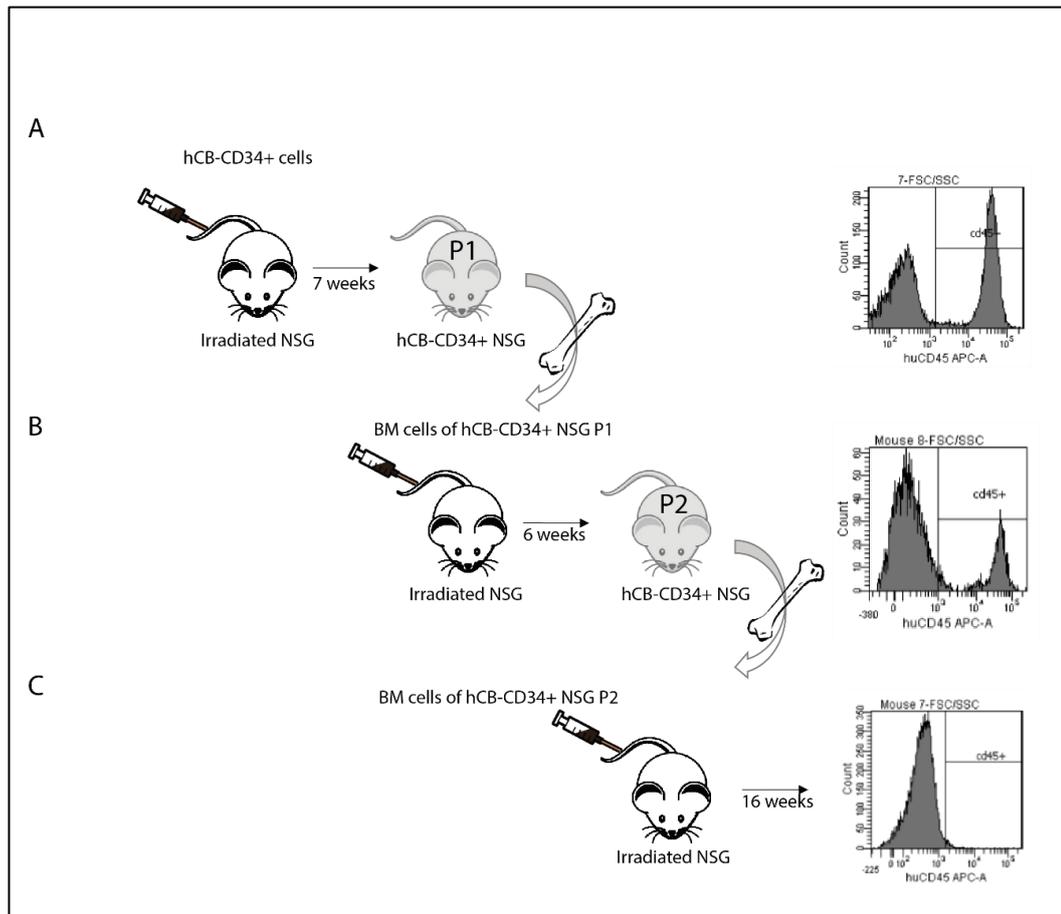
Figure 22. Generation of hCB-CD34+ NSG mice and propagation of hCB-CD34+ cells. NSG recipient mice were irradiated (1 Gy) prior transplantation. Engraftment of human cells has been evaluated via detection of human CD45+ cells in the PB of hCB-CD34+ NSG mice (flow cytometry analysis) **A)** engraftment at 7 weeks post transplant of hCB-CD34+ cells **B)** engraftment at 6 weeks post transplant of BM of P1 hCB-CD34+ NSG mice **C)** engraftment at 16 weeks post transplant of BM of P2 hCB-CD34+ NSG mice.

7.12 hCB-CD34+ NSG mice are accessible to human leukaemia growth

We investigated the accessibility of hCB-CD34+ NSG mice to tumour growth, following the development of the disease in hCB-CD34+ NSG mice upon human acute myeloid leukaemia (hAML) transplantation. Two different leukaemias from two AML patients have been intravenously injected in hCB-CD34+ NSG mice (1×10^6 leukaemia cells per mouse). Both control and hCB-CD34+ NSG mice transplanted with hAML developed leukaemia with comparable kinetics of disease (Figure 23A and 23B). The features of leukaemia, in terms of morphology of the blasts and organ infiltration by leukemic cells, did not show any difference between the two groups (Figure 23C and 23D). Similar behaviour has been observed in the hAMLs

developed in hCB-CD34+ humanized NSG mice when re-transplanted for an additional passage in NSG recipients (data not shown). These data suggest a complete accessibility of the hCB-CD34+ NSG mice to human leukaemia growth, most likely due to an inefficient recognition of the leukaemia by the human immune components developed in these mice.
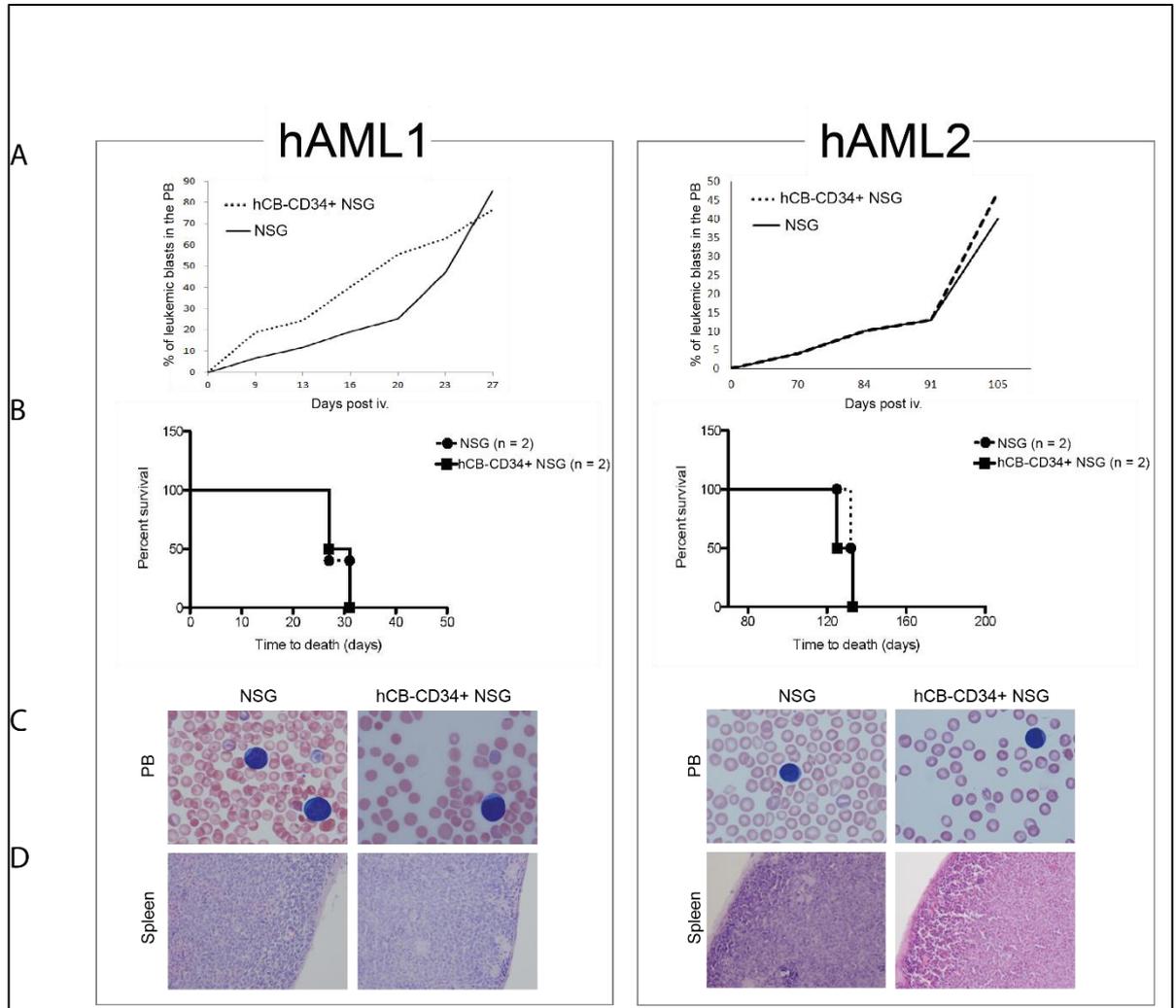
Figure 23. hAML transplant in hCB-CD34+ NSG recipients. Transplantability of two different hAMLs (hAML1 and hAML2) in hCB-CD34+ NSG and control NSG mice (at least two mice per group per each leukaemia). **A)** kinetics of the development of the disease represented as percentage of blasts in the PB. **B)** survival curve of humanized NSG vs control NSG mice transplanted with hAML1 and hAML2. **C)** leukemic blasts in blood smears of transplanted animals **D)** spleen architecture of transplanted animals.

7.13 hCB-CD34+ NSG mice do not support the maturation of human immune components

hCB-CD34+ NSG mice are completely accessible to hAML growth. In order to understand whether this is due to inability of human immune system developed in hCB-CD34+ NSG

mice to efficiently recognize and react to hAML presence, we performed FACS analysis of PB of hCB-CD34$^+$ NSG. We observed high occupancy of naïve T cells in the peripheral blood of hCB-CD34$^+$ NSG (CD45RA$^+$ = 42%, among human CD45$^+$ cells). On the other hand, we noticed very low amount of B cells (CD19$^+$ = 0.2%) and CD4$^+$ and CD8$^+$ (5.2% and 0.5%, respectively, among human CD45$^+$ cells). These data imply that the hCB-CD34$^+$ NSG mouse model develops a "primitive" human immune system. Moreover, in order to examine the functionality of human T cells in humanized context, we isolated human T cells from the spleen of hCB-CD34$^+$ NSG and performed *in vitro* CD3/CD28 activation. We then performed CFSE proliferation assay. We observed that human T cells of hCB-CD34$^+$ NSG do not proliferate upon canonical stimulation (none and 54% of CFSE^{low} CD3$^+$ cells from of hCB-CD34$^+$ NSG and from PB of a healthy human donor, respectively), suggesting the development of entirely non-functional T-cell compartment in the hCB-CD34$^+$ NSG mouse model.

8. DISCUSSION

In the last decade, a dual pro-tumoral role of the cell-cycle inhibitor p21 has been unrevealed. The initial discovery that p21 is critical for the re-transplantability of tumor suggested its central role in maintaining the self-renewal capacity of LSCs. The expression of leukaemia-associated oncogenes in HSCs was shown to induce DNA damage and activate a cellular response that relies on p21 which leads to reversible cell-cycle arrest, DNA damage repair and ultimately to perpetuation of LSCs pool[16]. Considering this evidence, a p21-dependent intrinsic mechanism by which LSCs handle DNA damage has been proposed. However, it remained unclear whether the self-renewal regulation of LSCs by p21 is solely a cell-autonomous process, or there are other p21-dependent cell-extrinsic mechanisms involved. The subsequent discovery that in the absence of p21 expression, leukaemia propagation depends on the immune system of the host, strongly suggested the existence of pro-tumoral cell-extrinsic mechanisms that rely on p21. It has been shown that upon transplantation of p21$^{-/-}$ leukaemia in immune-competent recipient, a potent anti-tumor CD4^{+} T-cell mediated immunological response is activated. Such CD4^{+} T-cell population can be used to vaccinate immune-deficient mice and protect them against AML development, emphasising the potency of p21-dependent immunological response. Therefore, in light of this evidence, p21 was suggested to play its pro-tumoral role not only by ensuring the unlimited self-renewal capacity to LSCs, but also by evading the exposure to the anti-tumor mechanism of the immune system. Yet, it remained unclear whether the two p21-dependent mechanisms could somehow co-operate, or the powerful anti-tumoral immunological response might overwrite the cell-autonomous effect.

All the experiments conducted to study the CD4^{+} T-cell mediated immunological mechanism of AML clearance have been performed transplanting p21$^{-/-}$ leukemic spleens as source of leukemic blasts. Although the major part of these leukemic spleens is composed of infiltrating p21$^{-/-}$ blasts (almost 90%), there are some cells of p21$^{-/-}$ splenic microenvironment remained. Those remained non-malignant cells, at the time of leukemic blast infiltration in

the spleen, depict the microenvironment of leukaemia. This aspect implied that also the cellular components that reside in $p21^{-/-}$ spleen exposed to the tumor (considered as $p21^{-/-}$ TME) could be crucial for eliciting the anti-tumor immunological response. Thus, in order to test our hypothesis, it was necessary to separate the $p21^{-/-}$ TME from leukemic blasts. However, the physical separation of the two components was not possible since they share the same myeloid-specific markers due to their common myeloid origin. Therefore, we set them apart by transplanting WT leukaemia in $p21^{-/-}$ mice (see Results 7.1.1). Although these mice develop leukaemia, their leukemic spleen consist of the majority of infiltrated WT leukemic blasts and cells of $p21^{-/-}$ splenic environment. Re-transplantation of such leukemic spleens, or transplantation of WT leukemic blasts along with healthy $p21^{-/-}$ spleen in immune-competent recipients resulted in the activation of the $CD4^{+}$ T-cell mediated immunological response against tumor (see Results 7.1.1 and 7.1.2). This demonstrated that indeed the lack of p21 expression in TME, independently on p21 status in the leukemic blast, is indispensable for activation of the immunological mechanism of tumor clearance. Interestingly, the analogous effect of $p21^{-/-}$ TME on mounting anti-tumor immunological response was observed also in FVB mouse strain (see Results 7.10.1 and 7.10.2) which suggested that the p21-dependent anti-tumoral response is not strain-specific. However, the p21-dependent anti-tumor immune response in FVB mice appear to be slightly distinct from the one in C57Bl6 mouse strain, since $p21^{-/-}$ FVB mice completely reject tumor (both leukaemia and breast cancer) (see Results 7.10.2). This could be due to crucial differences in the immune system between the two strains. While C57Bl6 mice activate Th1 immune response upon diverse stimuli, FVB mouse strain is known to activate Th2 response[58,108], which could result in different potency of the anti-leukemic immunological response. Moreover, we demonstrated that in FVB, p21 most likely co-operates with MLL-AF9 in leukaemogenesis (see Results 7.10.1), thus implying the existence of p21-dependent cell-autonomous mechanism also in this setting. Maybe the p21-dependent immunological mechanism in FVB strain has

the analogous bases to the one observed in C57Bl6, but the hierarchical organization of its players is set up differently, thus resulting in higher efficiency of the response.

The data obtained from the two mouse strains go in the same direction and contribute to demonstrate for the first time that in the absence of p21, splenic TME is critical for mounting an immunological response against the tumor. Considering the fact that the anti-tumor immunological response is activated exclusively in the p21$^{-/-}$ TME context, we assumed the existence of crucial biological differences between p21$^{-/-}$ and WT splenic TMEs. Actually, the quantification of the ratio of splenic primary follicles and germinal centers, which are indicators of splenic activation, both under steady state and upon leukaemia challenge, demonstrated that under basal conditions, p21$^{-/-}$ spleens are immunologically more active and able to respond to tumor challenge with a faster kinetics compared to WT (see Result 7.2). Those p21$^{-/-}$ spleens originate from p21$^{-/-}$ C57Bl6 mice in which, due to the lack of p21, memory T cells hyperproliferate and eventually lose tolerance to autoantigens[23]. However, the loss of self-tolerance is mild in these mice and does not result in severe lupus-like phenotype[23]. The subpathological autoimmunity in these mice could explain the observed "hyper-activated" state of p21$^{-/-}$ splenic environment under steady conditions. Such p21$^{-/-}$ splenic environment, after exposure to leukaemia, is able to elicit the immunological response against tumor, strongly suggesting the presence of key mediators of the anti-tumor immunological response in p21$^{-/-}$ splenic TME. The analyses of T-cell compartments in p21$^{-/-}$ and WT splenic environment under steady state and upon leukaemia challenge excluded the involvement of T cells in the early activation of the p21-dependent immune response (see Results 7.3). This evidence implied that the anti-leukemic CD4^{+} T-cell mediated immunological response, triggered by p21$^{-/-}$ splenic environment, occurs later in the time, rather than shortly after tumor challenge. This is also supported by the fact that in the presence of p21$^{-/-}$ leukemic spleen in immune-competent host, the activation of "killing" CD4^{+} T-cell population occurs 15 days post leukaemia exposure.

Taking into consideration that along the spleen, BM is recognized as TME in haematological malignancies, we investigated whether the ability of p21^{-/-} TME to trigger anti-leukemic immune response could be associated also to the BM. The concomitant transplantation of WT leukaemia and p21^{-/-} BM in immune-competent mice, similarly to experiment of p21^{-/-} spleen transfer, vaccinated from leukaemia development (see Results 7.1.2). This implied that the key p21^{-/-} mediator of the anti-tumor immunological response must be a cellular component present both in spleen and BM. Considering that the p21-dependent mechanism of cytotoxic CD4^{+} T-cell activation fully relies on MHC II expression (see paragraph 5.2.3), our cell of interest must be a professional antigen-presenting cell present in the BM and in the spleen. We assumed that this p21^{-/-} professional APC could efficiently present tumor-specific antigen on MHC II and activate CD4^{+} T-cell population to eradicate the tumor. Macrophages are considered as professional APCs that constitutively express high levels of MHC II molecules, antigen-processing machinery and co-stimulatory molecules and there is evidence of their ability to activate naïve CD4^{+} T cells in an antigen-specific manner.

In order to unravel the crucial biological differences between WT and p21^{-/-} macrophages that render the latter able to mount anti-tumor immune response, we investigated the behaviour of p21^{-/-} and WT macrophages in the presence of different stimuli. The fact that the lack of p21 expression in diverse cells results in DNA damage accumulation[4] led to hypothesize that p21^{-/-} splenic macrophages could be hyper-damaged and that this feature induces their special anti-tumoral biological behaviour. By exposing splenic macrophages to chronic and acute source of DNA damage, we demonstrated that independently on their p21 status, splenic macrophages express fully resistant phenotype to DNA damage (see Results 7.5.2). This evidence suggested a different mechanism of DNA damage handling in macrophages compared to other cells of the tissue, which however, does not rely on p21. In fact, our data correlate with other reports on p21-independent macrophage DNA repair mechanisms[109], thus implying that the crucial biological differences between p21^{-/-} and WT macrophages do not have their basis in mechanisms of DNA-damage handling.

We then investigated whether the lack of p21 in macrophages induces a particular response to unspecific or tumor-specific stimuli, that would eventually result in a different biological behaviour of p21$^{-/-}$ macrophages. By generating BMDMs from WT and p21$^{-/-}$ BM and exposing them to unspecific stimuli, such as IFN-γ and LPS *in vitro*, we demonstrated that both WT and p21$^{-/-}$ BMDMs acquire comparable activation phenotype (see Results 7.5.1). These data implied that their responsiveness to unspecific stimuli does not depend on p21 (see Results 7.5.1). On the other hand, p21$^{-/-}$ BMDMs were able to mount anti-leukemic immune response *in vivo* (see Results 7.4.2), implying that BMDMs respond exclusively to tumor stimuli in a p21-dependent manner. In addition to this evidence, the responsiveness of splenic macrophages to tumor exposure *in vivo* was also shown to rely on p21 (see Results 7.4.1). Steady state p21$^{-/-}$ splenic macrophages express a hyper-active inflammatory phenotype, hallmarked by up-regulation of MHC II, and it ensures a faster response to tumor presence (see Results 7.4.1). This evidence coincides with greater immunological responsiveness of p21$^{-/-}$ spleen upon tumor stimulus, confirming the critical involvement of p21$^{-/-}$ macrophages in anti-tumor response. The analogous p21-dependent splenic macrophage activation upon tumor stimulus was observed also in the FVB mouse strain. Here we showed that in the absence of p21, splenic macrophages engage an inflammatory phenotype that could possess altered antigen-processing and antigen-presenting mechanisms, inducing durable CD4$^+$ T-cell response against tumor, yet the underlying mechanisms still remain unclear. In addition to our data, there are other studies supporting the critical role of p21 in promoting macrophage hypo-responsive state[110]. In particular, upon LPS stimulation, p21$^{-/-}$ peritoneal macrophages were shown to produce increased levels of pro-inflammatory cytokines when compared to WT macrophages, suggesting that p21 negatively regulates macrophage inflammatory response by inducing macrophage immunosuppression[110].

In light of the evidence that p21$^{-/-}$ APC is key mediator of the potent anti-tumor immune response, it was necessary to fully characterize this APC present in p21$^{-/-}$ TME. The phenotypical characterization of a discrete cellular component from tissue mainly relies on the

specific surface markers expressed on the cell of interest. Initially, we attempted to identify and extract splenic macrophages using CD11b and CD11c markers. Although these markers are expressed mainly on macrophages (CD11b) or DCs (CD11c), their diverse subpopulations can share both markers, thus causing difficulties in their characterization. In fact, *in vivo* transplantation of either $p21^{-/-}$ CD11b$^+$ or CD11c$^+$ cells along with WT leukaemia in immune-competent mice did not result in the activation of the CD4$^+$ T-cell mediated immune response (see Result 7.6.1). These data demonstrated that the key $p21^{-/-}$ player cannot be distinguished by the sole expression of CD11b or CD11c marker, thus suggesting that the $p21^{-/-}$ mediator might be a discrete subpopulation of $p21^{-/-}$ macrophages and in order to characterize it, additional cellular markers had to be used.

Additional approach to discriminate splenic macrophage subpopulations is based on their ontogeny or spatial position in the spleen. Macrophages in the spleen can derive from embryonic precursors or monocytes, or they can be of mixed origin, and their origin-dependent functions are still not fully clear[102]. In addition, different subpopulations of macrophages are found in specific niches of the spleen. Metallophilic, marginal zone, red and white pulp macrophages are phenotypically distinguishable and they possess specific immunological functions[103]. However, we observed very low percentage of these subpopulations in the spleen, independently on p21 expression (see Results 7.6.2), which implied that this approach is not optimal for detection of distinctive macrophage subpopulation in $p21^{-/-}$ TME and that different methodologies of identification should be applied.

Therefore, in order to visualize the rare $p21^{-/-}$ macrophage subpopulation in the splenic environment, we performed IHC analyses of "Pan-macrophage" markers, Iba1 and CD68, on spleens under basal conditions or post tumor challenge. The constitutive expression of Iba1 in splenic macrophages independently on p21 allowed us to exclude its usage for this purpose. On the other hand, the increased expression of activation marker CD68 in $p21^{-/-}$ macrophages, both under steady state conditions and upon tumor challenge (see Results 7.6.2), confirmed the hyper-activated state of $p21^{-/-}$ macrophages at basal conditions and suggested

faster and different recruitment of CD68^{+} macrophages in p21^{-/-} splenic environment upon tumor stimulus.

Such faster recruitment of CD68^{+} macrophages in p21^{-/-} splenic environment to tumor stimuli would ultimately result in efficient mounting of the potent immunological response against tumor. Recently, a new subpopulation of CD68^{+} TAMs has been discovered in the TME of patients with non-small cell lung cancer[76]. These TAMs retain Fe (iTAMs) and, opposite of majority of TAM populations, perform anti-tumoral functions[76]. Considering this evidence, we analysed p21^{-/-} splenic macrophages for their iron content. Independently on p21 expression, mainly red pulp macrophages contain Fe particles (see Results 7.7.1), which coincide with other scientific reports on red pulp macrophages and their crucial role in maintaining Fe homeostasis by recycling Fe from senescent RBCs[111]. Interestingly, the exposure to tumor promoted the migration of p21^{-/-} Fe-loaded macrophages inside primary follicles (see Results 7.7.1). Considering the fact that the antigen-presentation by APCs to T cells occurs in splenic primary follicles, our data strongly imply that in response to tumor presence, p21^{-/-} Fe-loaded macrophages are recruited to splenic primary follicles in order to efficiently present tumor-specific antigen to the T-cell compartment. Strikingly, such p21^{-/-} Fe-loaded macrophage subpopulation is also positive for CD68 (see Results 7.7.2), clearly demonstrating the appearance of iTAMs in p21^{-/-} spleen upon tumor challenge. Interestingly, we identified the iTAMs also in the p21^{-/-} TME of lung cancer (see Results 7.7.2).

Another aspect that characterizes macrophages and correlates to Fe-retention is the M1/M2 polarization status. Polarization of macrophages is known to either dictate or to be dictated by the expression of genes involved in iron metabolism[67]. A grey scale of M1/M2 intermediates exists and the levels of Fe-content can strongly influence the shift towards M1 or M2 phenotype. By modulating systemic iron content *in vivo*, we have been able to partially manipulate splenic macrophage polarization. In the absence of p21, splenic macrophages confer a mild M1-like phenotype upon systemic iron depletion (see Results 7.8.1), while the iron-overload does not affect the expression profile of macrophages, independently on p21 status

(see Results 7.8.2). In the absence of iron in the environment, macrophages tend to retain iron and the retention is further enhanced by p21 absence, inducing M1-like phenotype. In line with our data, a study of Rackov and colleagues demonstrated that the lack of p21 in peritoneal macrophages induced an M1-like phenotype upon LPS stimulation[110]. Interestingly, iTAMs present in the TME of NSCLC were also reported to be M1-polarized[76]. Our data strongly imply that the absence of p21 renders macrophages more prone to M1 phenotype, both under Fe-depletion and tumor-exposure challenge. Therefore, we can conclude that in the absence of p21 and upon tumor challenge, an iTAM population is recruited from the blood stream to the site of tumor infiltration and that this population is M1-polarized with the anti-tumoral activity.

By identifying iTAMs as essential trigger of the immunological response against the tumor in mice, we delineated the cellular mechanism of p21-dependent $CD4^+$ T-cell mediated tumor clearance. Translating the discovered anti-tumor immunological mechanism into human context is of great importance as it would lead to the development of efficient immune-therapies for cancer patients. Thus, it was necessary to understand whether the anti-tumoral T cell-mediated immune response triggered by $p21^{-/-}$ iTAMs occurs in humans. In order to do so, it was crucial to establish a proper humanized mouse model, containing human immune system. Transplantation of human $CD34^+$ cells originated from the cord blood of healthy donors in immune-deficient mice lead to successful engraftment of these cells and generation of human immune components in these mice (see Results 7.11.1). Importantly, we demonstrated that human $CD34^+$ cells can be propagated, yet only after one passage in NSG recipients (see Results 7.11.2). This evidence suggested that although $hCD34^+$ cells possess stimulated self-renewal capacity upon re-transplantation, they are pushed to proliferate and undergo functional exhaustion in NSG mice, yet the underlying molecular mechanisms still remain unclear.

Although hCB-CD34$^+$ NSG mice developed all the components of human immunity (see Results 7.13), they were completely accessible to the growth of human leukaemia (see Results 7.12). This could be due to an inefficient recognition of the leukaemia by the human immune system developed in these mice. In fact, the phenotype of the human immune system in hCB-CD34$^+$ NSG resembled a "primitive" one, and with the highest occupancy of naïve T cells (see Results 7.13). The naïve human T cells were completely unresponsive to canonical stimulation (see Results 7.13). This evidence suggests that hCB-CD34$^+$ NSG are transient and incomplete carriers of the human immune system and are an insufficient model to study interactions between human immune system and human cancer. Despite the fact that this model develops all the components of human immunity, we did not find the "window" of accessibility to cancer growth where there is a balance between response of the immune system and escape of the tumor. Actually, the hCB-CD34$^+$ NSG is a fully accessible system to human tumor growth, comparable to a xenograft model in the absence of the human immune system and can be definitively abandoned as tool for translational studies of leukaemia immuno-treatments.

Thus, further improvements are needed in order to achieve an ultimate humanized mouse model that offers an acceptable window of response/escape where to study interactions between the human immune system and human cancer in not-fully-compatible conditions. Development of such model will allow to understand whether the anti-tumor immunological response elicited by p21$^{-/-}$ iTAMs is conserved also in humans. This part of our work is of great importance for other scientists since it facilitates choosing the right humanized mouse model to study and develop immune-therapies against leukaemia.

It is already known that immune system is able to recognize malignant cells and activate clearance responses. However, cancer cells are often capable of evading immune surveillance mechanisms, allowing tumor progression. Tumor microenvironment has emerged as one of the key factors supporting tumor escape and growth, due to its mainly inhibitory effect

on the host's immune system. Therefore, manipulation of the components of TME and dissection of poorly understood cellular and molecular mechansims of tumor-escape would allow development of active cancer immunotherapies.

p21 has been previously proposed to play a pro-tumoral role by evading the surveillance mechanisms of the immune system (see paragraph 5.2.1). A CD4$^+$ T-cell mediated immunological response is activated in the presence of p21$^{-/-}$ leukemic spleen (see paragraph 5.2.2 and 5.2.4). Yet, until now, the cellular mechanism underneath this potent anti-tumor immunological response has never been described before.

In this work, we unrevealed the crucial role of p21$^{-/-}$ tumor microenvironment in triggering anti-tumor immunological response. We identified for the first time p21$^{-/-}$ iTAMs present in the tumor microenvironment as key mediators of a potent immunological mechanism of cancer clearance. A fine manipulation of p21 expression together with mechanisms of Fe-handling in macrophages in the microenvironment of diverse tumors would enhance their antigen-presentation functions and allow efficient activation of T cells that would ultimately clear the tumors. Although the molecular mechanisms by which iTAMs efficiently activate powerful and durable anti-cancer CD4$^+$ T-cell response in the absence of p21 remain poorly understood, our discovery is of great importance since it establishes the basis to design efficient vaccine against cancer. Development of such vaccines will represent an immense step in the field of immune-oncology, as it will allow less toxic and more efficient immune-therapies for cancer patients.

While repeating the above-mentioned experiments, we encountered problems with the reproducibility of some of them, due to the unexpected loss of the biological phenotype of p21$^{-/-}$ C57Bl6 and p21$^{-/-}$ PRKi mice. In particular, p21$^{-/-}$ PRKi mice did not develop leukaemias as expected (see Results 7.9 and also ref. 16), and p21$^{-/-}$ C57Bl6 mice did not exhibit the well-established protective phenotype against leukaemias (see Results 7.9). Initially, we hypothesized that the observed absence of the main traits of p21$^{-/-}$ phenotype could be due to

possible appearance of new, untraceable genetic variants in p21$^{-/-}$ mice. These genetic modifications might have influenced the immune system of p21$^{-/-}$ mice and, consecutively, their ability to mount an anti-leukemic immune response. To test this hypothesis, we re-generated our p21$^{-/-}$ mouse colonies. However, we did not observe restoration of the immunological phenotype of these mice. These observations led us to hypothesize the existence of environmental changes that might have altered the immunological status of these mice (for example changes in the gut microbiota composition). Along the same line, recently, we noticed the re-occurrence of leukaemias in the p21$^{-/-}$ PRKi mice, as previously observed. These continuous alterations in the biological phenotype of p21$^{-/-}$ mice strongly support our hypothesis of the existence of environmental factors and their impact on the immunity of these animals, which is at the moment under evaluation. In-depth studies of the environmental factors would allow for the possibility to indirectly manipulate the immunity of these mice towards a potent anti-tumoral phenotype.

Importantly, as described before, we observe a protective biological phenotype of p21$^{-/-}$ mice of a different genetic background (FVB). This evidence strongly confirms the presence of a potent anti-tumoral immune response in p21-null context and add to the solidity of the data demonstrated in this work.

9. REFERENCES

1.   Karimian, A., Ahmadi, Y. & Yousefi, B. Multiple functions of p21 in cell cycle, apoptosis and transcriptional regulation after DNA damage. *DNA Repair* **42**, 63–71 (2016).

2.   Cayrol, C., Knibiehler, M. & Ducommun, B. p21 binding to PCNA causes G1 and G2 cell cycle arrest in p53-deficient cells. *Oncogene* **16,** 311-320 (1998).

3.   Cazzalini, O., Scovassi, A. I., Savio, M., Stivala, L. A. & Prosperi, E. Multiple roles of the cell cycle inhibitor p21CDKN1A in the DNA damage response. *Mutat. Res.* **704**, 12–20 (2010).

4.   Georgakilas, A. G., Martin, O. A. & Bonner, W. M. p21: A Two-Faced Genome Guardian. *Trends Mol. Med.* **23**, 310–319 (2017).

5.   Barboza, J. A., Liu, G., Ju, Z., El-Naggar, A. K. & Lozano, G. p21 delays tumor onset by preservation of chromosomal stability. *Proc. Natl. Acad. Sci.* **103**, 19842–19847 (2006).

6.   Martın-Caballero, J., Flores, J. M., Garcıa-Palencia, P. & Serrano, M. Tumor Susceptibility of p21Waf1/Cip1-deficient Mice. *Cancer Res.* **61,** 6234-6238 (2001).

7.   Abbas, T. & Dutta, A. p21 in cancer: intricate networks and multiple activities. *Nat. Rev. Cancer* **9**, 400–414 (2009).

8.   Trakala, M. *et al.* Regulation of macrophage activation and septic shock susceptibility *via* p21(WAF1/CIP1): Innate immunity. *Eur. J. Immunol.* **39**, 810–819 (2009).

9.   Gartel, A. L. Is p21 an oncogene? *Mol. Cancer Ther.* **5**, 1385–1386 (2006).

10.   De la Cueva, E. *et al.* Tumorigenic activity of p21Waf1/Cip1 in thymic lymphoma. *Oncogene* **25**, 4128 (2006).

11.   Okuma, A., Hanyu, A., Watanabe, S. & Hara, E. p16Ink4a and p21Cip1/Waf1 promote tumour growth by enhancing myeloid-derived suppressor cells chemotaxis. *Nat. Commun.* **8**, 2050 (2017).

12.   Shenghui, H., Nakada, D. & Morrison, S. J. Mechanisms of Stem Cell Self-Renewal. *Annu. Rev. Cell Dev. Biol.* **25**, 377–406 (2009).

13.   Verga Falzacappa, M. V., Ronchini, C., Reavie, L. B. & Pelicci, P. G. Regulation of self-renewal in normal and cancer stem cells: Role of stem cell self-renewal in cancer. *FEBS J.* **279**, 3559–3572 (2012).

14.   Cicalese, A. *et al.* The Tumor Suppressor p53 Regulates Polarity of Self-Renewing Divisions in Mammary Stem Cells. *Cell* **138**, 1083–1095 (2009).

15.   Insinga, A. *et al.* DNA damage in stem cells activates p21, inhibits p53, and induces symmetric self-renewing divisions. *Proc. Natl. Acad. Sci.* **110**, 3931 (2013).

16.   Viale, A. *et al.* Cell-cycle restriction limits DNA damage and maintains self-renewal of leukaemia stem cells. *Nature* **457**, 51–56 (2009).

17.   Matsumoto, A. *et al.* p57 Is Required for Quiescence and Maintenance of Adult Hematopoietic Stem Cells. *Cell Stem Cell* **9**, 262–271 (2011).

18.   Zou, P. *et al.* p57Kip2 and p27Kip1 Cooperate to Maintain Hematopoietic Stem Cell Quiescence through Interactions with Hsc70. *Cell Stem Cell* **9**, 247–261 (2011).

19.   Cheng, T., Rodrigues, N., Dombkowski, D., Stier, S. & Scadden, D. T. Stem cell repopulation efficiency but not pool size is governed by p27kip1. *Nat. Med.* **6**, 1235 (2000).

20.   Cheng, T. Hematopoietic Stem Cell Quiescence Maintained by p21cip1/waf1. *Science* **287**, 1804–1808 (2000).

21.   Minucci, S. *et al.* PML-RAR induces promyelocytic leukemias with high efficiency following retroviral gene transfer into purified murine hematopoietic progenitors. *Blood* **100**, 2989–2995 (2002).

22.   Gaud, G., Lesourne, R. & Love, P. E. Regulatory mechanisms in T cell receptor signalling. *Nat. Rev. Immunol.* **18,** 485-497 (2018).

23.   Arias, C. F. *et al.* p21CIP1/WAF1 Controls Proliferation of Activated/Memory T Cells and Affects Homeostasis and Memory T Cell Responses. *J. Immunol.* **178**, 2296–2306 (2007).

24.   Rachel R. Caspi. Immunotherapy of autoimmunity and cancer: the penalty for success. *Nat. Rev. Immunol.* **8**, 970–976 (2008).

25.   Giat, E., Ehrenfeld, M. & Shoenfeld, Y. Cancer and autoimmune diseases. *Autoimmun. Rev.* **16**, 1049–1057 (2017).

26.   Franks, A. L. Multiple Associations Between a Broad Spectrum of Autoimmune Diseases, Chronic Inflammatory Diseases and Cancer. *Anticancer Res.* **32,** 1119-11136 (2012).

27.   Simon, T. A., Thompson, A., Gandhi, K. K., Hochberg, M. C. & Suissa, S. Incidence of malignancy in adult patients with rheumatoid arthritis: a meta-analysis. *Arthritis Res. Ther.* **17**, 212 (2015).

28.   Amos, S. M. *et al.* Autoimmunity associated with immunotherapy of cancer. *Blood* **118**, 499–509 (2011).

29.   June, C. H., Warshauer, J. T. & Bluestone, J. A. Is autoimmunity the Achilles' heel of cancer immunotherapy? *Nat. Med.* **23**, 540–547 (2017).

30.   Attia, P. *et al.* Autoimmunity Correlates With Tumor Regression in Patients With Metastatic Melanoma Treated With Anti–Cytotoxic T-Lymphocyte Antigen-4. *J. Clin. Oncol.* **23**, 6043–6053 (2005).

31.   Beck, K. E. *et al.* Enterocolitis in Patients With Cancer After Antibody Blockade of Cytotoxic T-Lymphocyte–Associated Antigen 4. *J. Clin. Oncol.* **24**, 2283–2289 (2006).

32.   Santiago-Raber, M.-L. *et al.* Role of Cyclin Kinase Inhibitor p21 in Systemic Autoimmunity. *J. Immunol.* **167**, 4067–4074 (2001).

33.   Kim, K. *et al.* A regulatory SNP at position -899 in CDKN1A is associated with systemic lupus erythematosus and lupus nephritis. *Genes Immun.* **10,** 482-486 (2009).

34.   Smolen, J. S. *et al.* HLA-DR antigens in systemic lupus erythematosus: association with specificity of autoantibody responses to nuclear antigens. *Ann. Rheum. Dis.* **46**, 457–462 (1987).

35.   Kaul, A. *et al.* Systemic lupus erythematosus. *Nat. Rev. Dis. Primer* **2**, 16039 (2016).

36.   Balomenos, D. *et al.* The cell cycle inhibitor p21 controls T-cell proliferation and sex-linked lupus development. *Nat. Med.* **6**, 171–176 (2000).

37.   Hanahan, D. & Weinberg, R. A. Hallmarks of Cancer: The Next Generation. *Cell* **144**, 646–674 (2011).

38.   Whiteside, T. L. The tumor microenvironment and its role in promoting tumor growth. *Oncogene* **27**, 5904–5912 (2008).

39.   Martin, M., Wei, H. & Lu, T. Targeting microenvironment in cancer therapeutics. *Oncotarget* **7**, 52575-52583 (2016).

40.   Binnewies, M. *et al.* Understanding the tumor immune microenvironment (TIME) for effective therapy. *Nat. Med.* **24**, 541–550 (2018).

41.   Wang, M. *et al.* Role of tumor microenvironment in tumorigenesis. *J. Cancer* **8**, 761–773 (2017).

42.   Yang, L. & Zhang, Y. Tumor-associated macrophages: from basic research to clinical application. *J. Hematol. Oncol.* **10**, 58 (2017).

43.   Gabrilovich, D. I., Ostrand-Rosenberg, S. & Bronte, V. Coordinated regulation of myeloid cells by tumours. *Nat. Rev. Immunol.* **12**, 253–268 (2012).

44.   von Boehmer, H. & Daniel, C. Therapeutic opportunities for manipulating TReg cells in autoimmunity and cancer. *Nat. Rev. Drug Discov.* **12**, 51–63 (2013).

45.   Zitvogel, L., Tesniere, A. & Kroemer, G. Cancer despite immunosurveillance: immunoselection and immunosubversion. *Nat. Rev. Immunol.* **6**, 715 (2006).

46.   Gajewski, T. F., Schreiber, H. & Fu, Y.-X. Innate and adaptive immune cells in the tumor microenvironment. *Nat. Immunol.* **14**, 1014–1022 (2013).

47.   Elpek, K. G. *et al.* The Tumor Microenvironment Shapes Lineage, Transcriptional, and Functional Diversity of Infiltrating Myeloid Cells. *Cancer Immunol. Res.* **2**, 655–667 (2014).

48.   Sinha, P., Clements, V. K. & Ostrand-Rosenberg, S. Reduction of Myeloid-Derived Suppressor Cells and Induction of M1 Macrophages Facilitate the Rejection of Established Metastatic Disease. *J. Immunol.* **174**, 636–645 (2005).

49.   Liu, C. *et al.* Expansion of spleen myeloid suppressor cells represses NK cell cytotoxicity in tumor-bearing host. *Blood* **109**, 4336–4342 (2007).

50.   Biswas, S. K. & Mantovani, A. Macrophage plasticity and interaction with lymphocyte subsets: cancer as a paradigm. *Nat. Immunol.* **11**, 889–896 (2010).

51.   Sica, A. & Mantovani, A. Macrophage plasticity and polarization: in vivo veritas. *J. Clin. Invest.* **122**, 787–795 (2012).

52.   Mantovani, A., Sozzani, S., Locati, M., Allavena, P. & Sica, A. Macrophage polarization: tumor-associated macrophages as a paradigm for polarized M2 mononuclear phagocytes. *Trends Immunol.* **23,** 549-555 (2002).

53.   Laoui, D. *et al.* Tumor Hypoxia Does Not Drive Differentiation of Tumor-Associated Macrophages but Rather Fine-Tunes the M2-like Macrophage Population. *Cancer Res.* **74**, 24–30 (2014).

54.   Petrova, V., Annicchiarico-Petruzzelli, M., Melino, G. & Amelio, I. The hypoxic tumour microenvironment. *Oncogenesis* **7**, 10 (2018).

55. Henze, A.-T. & Mazzone, M. The impact of hypoxia on tumor-associated macrophages. *J. Clin. Invest.* **126**, 3672–3679 (2016).

56. Quail, D. F. & Joyce, J. A. Microenvironmental regulation of tumor progression and metastasis. *Nat. Med.* **19**, 1423–1437 (2013).

57. Wyckoff, J. B. *et al.* Direct Visualization of Macrophage-Assisted Tumor Cell Intravasation in Mammary Tumors. *Cancer Res.* **67**, 2649–2656 (2007).

58. Mills, C. D., Kincaid, K., Alt, J. M., Heilman, M. J. & Hill, A. M. M-1/M-2 Macrophages and the Th1/Th2 Paradigm. *J. Immunol.* **164**, 6166–6173 (2000).

59. Martinez, F. O. & Gordon, S. The M1 and M2 paradigm of macrophage activation: time for reassessment. *F1000Prime Rep.* **6**, 13 (2014).

60. Aras, S. & Zaidi, M. R. TAMeless traitors: macrophages in cancer progression and metastasis. *Br. J. Cancer* **117**, 1583–1591 (2017).

61. Solinas, G., Germano, G., Mantovani, A. & Allavena, P. Tumor-associated macrophages (TAM) as major players of the cancer-related inflammation. *J. Leukoc. Biol.* **86**, 1065–1073 (2009).

62. Noy, R. & Pollard, J. W. Tumor-Associated Macrophages: From Mechanisms to Therapy. *Immunity* **41**, 49–61 (2014).

63. Wynn, T. A., Chawla, A. & Pollard, J. W. Macrophage biology in development, homeostasis and disease. *Nature* **496**, 445 (2013).

64. Mills, C. D., Shearer, J., Evans, R. & Caldwell, M. D. Macrophage arginine metabolism and the inhibition or stimulation of cancer. *J Immunol.* **149,** 2709-2714 (1992).

65. Ruffell, B. & Coussens, L. M. Macrophages and Therapeutic Resistance in Cancer. *Cancer Cell* **27**, 462–472 (2015).

66. Mantovani, A. *et al.* The chemokine system in diverse forms of macrophage activation and polarization. *Trends Immunol.* **25**, 677–686 (2004).

67. Jung, M., Mertens, C. & Brüne, B. Macrophage iron homeostasis and polarization in the context of cancer. *Immunobiology* **220**, 295–304 (2015).

68. Soares, M. P. & Hamza, I. Macrophages and Iron Metabolism. *Immunity* **44**, 492–504 (2016).

69. Corna, G. *et al.* Polarization dictates iron handling by inflammatory and alternatively activated macrophages. *Haematologica* **95**, 1814–1822 (2010).

70. Recalcati, S. *et al.* Differential regulation of iron homeostasis during human macrophage polarized activation. *Eur. J. Immunol.* **40**, 824–835 (2010).

71. Beatty, G. L. *et al.* CD40 Agonists Alter Tumor Stroma and Show Efficacy Against Pancreatic Carcinoma in Mice and Humans. *Science* **331**, 1612–1616 (2011).

72. Almatroodi, S. A., McDonald, C. F., Darby, I. A. & Pouniotis, D. S. Characterization of M1/M2 Tumour-Associated Macrophages (TAMs) and Th1/Th2 Cytokine Profiles in Patients with NSCLC. *Cancer Microenviron.* **9**, 1–11 (2016).

73. Ohri, C. M., Shikotra, A., Green, R. H., Waller, D. A. & Bradding, P. Macrophages within NSCLC tumour islets are predominantly of a cytotoxic M1 phenotype associated with extended survival. *Eur. Respir. J.* **33**, 118–126 (2009).

74.   Pollard, J. W. Tumour-educated macrophages promote tumour progression and metastasis. *Nat. Rev. Cancer* **4**, 71 (2004).

75.   Zaidi, M. R. *et al.* Interferon-γ links ultraviolet radiation to melanomagenesis in mice. *Nature* **469**, 548 (2011).

76.   Costa da Silva, M. *et al.* Iron Induces Anti-tumor Activity in Tumor-Associated Macrophages. *Front. Immunol.* **8**, 1479 (2017).

77.   Li, Z.-W. & Dalton, W. S. Tumor microenvironment and drug resistance in hematologic malignancies. *Blood Rev.* **20**, 333–342 (2006).

78.   Korn, C. & Méndez-Ferrer, S. Myeloid malignancies and the microenvironment. *Blood* **129**, 811–822 (2017).

79.   Bakker, E., Qattan, M., Mutti, L., Demonacos, C. & Krstic-Demonacos, M. The role of microenvironment and immunity in drug response in leukemia. *Biochim. Biophys. Acta BBA - Mol. Cell Res.* **1863**, 414–426 (2016).

80.   Curran, E. K., Godfrey, J. & Kline, J. Mechanisms of Immune Tolerance in Leukemia and Lymphoma. *Trends Immunol.* **38**, 513–525 (2017).

81.   Dhodapkar, M. V., Krasovsky, J. & Olson, K. T cells from the tumor microenvironment of patients with progressive myeloma can generate strong, tumor-specific cytolytic responses to autologous, tumor-loaded dendritic cells. *Proc. Natl. Acad. Sci.* **99**, 13009–13013 (2002).

82.   Shaked, Y. The splenic microenvironment is a source of proangiogenesis/inflammatory mediators accelerating the expansion of murine erythroleukemic cells. *Blood* **105**, 4500–4507 (2005).

83.   Ma, S. *et al.* Notch1-induced T cell leukemia can be potentiated by microenvironmental cues in the spleen. *J. Hematol. Oncol.J Hematol Oncol* **7**, 71 (2014).

84.   Gätjen, M. *et al.* Splenic Marginal Zone Granulocytes Acquire an Accentuated Neutrophil B-Cell Helper Phenotype in Chronic Lymphocytic Leukemia. *Cancer Res.* **76**, 5253–5265 (2016).

85.   Shultz, L. D., Ishikawa, F. & Greiner, D. L. Humanized mice in translational biomedical research. *Nat. Rev. Immunol.* **7**, 118 (2007).

86.   Walsh, N. C. *et al.* Humanized Mouse Models of Clinical Disease. *Annu. Rev. Pathol. Mech. Dis.* **12**, 187–215 (2017).

87.   Wiekmeijer, A.-S. *et al.* Sustained Engraftment of Cryopreserved Human Bone Marrow CD34 $^+$ Cells in Young Adult NSG Mice. *BioResearch Open Access* **3**, 110–116 (2014).

88.   Cytokine Stimulation of Multilineage Hematopoiesis from Immature Human Cells Engrafted in SCID Mice Author(s): Tsvee Lapidot, Francoise Pflumio, Monica Doedens, Barbara Murdoch, Douglas E. Williams and John E. Dick. *Sci. New Ser.* **255**, 1137–1141 (1992).

89.   Shultz, L. D. *et al.* Multiple defects in innate and adaptive immunologic function in NOD/LtSz-scid mice. *J. Immunol.* **154**, 180 (1995).

90.   Shultz, L. D. *et al.* Human Lymphoid and Myeloid Cell Development in NOD/LtSz-scid IL2Rγ^{null} Mice Engrafted with Mobilized Human Hemopoietic Stem Cells. *J. Immunol.* **174**, 6477 (2005).

91.	Ito, M. NOD/SCID/gamma cnull mouse: an excellent recipient mouse model for engraftment of human cells. *Blood* **100**, 3175–3182 (2002).

92.	Ishikawa, F. Development of functional human blood and immune systems in NOD/SCID/IL2 receptor chainnull mice. *Blood* **106**, 1565–1573 (2005).

93.	King, M. A. *et al.* Human peripheral blood leucocyte non-obese diabetic-severe combined immunodeficiency interleukin-2 receptor gamma chain gene mouse model of xenogeneic graft- *versus* -host-like disease and the role of host major histocompatibility complex. *Clin. Exp. Immunol.* **157**, 104–118 (2009).

94.	Greenblatt, M. B. *et al.* Graft versus Host Disease in the Bone Marrow, Liver and Thymus Humanized Mouse Model. *PLoS ONE* **7**, e44664 (2012).

95.	Watanabe, Y. *et al.* The analysis of the functions of human B and T cells in humanized NOD/shi-scid/γcnull (NOG) mice (hu-HSC NOG mice). *Int. Immunol.* **21**, 843–858 (2009).

96.	Norelli, M. *et al.* Monocyte-derived IL-1 and IL-6 are differentially required for cytokine-release syndrome and neurotoxicity due to CAR T cells. *Nat. Med.* **24**, 739–748 (2018).

97.	Vinchi, F. *et al.* Hemopexin therapy reverts heme-induced proinflammatory phenotypic switching of macrophages in a mouse model of sickle cell disease. *Blood* **127**, 473–486 (2016).

98.	Allen, C. D. C., Okada, T. & Cyster, J. G. Germinal-Center Organization and Cellular Dynamics. *Immunity* **27**, 190–202 (2007).

99.	Coffey, F., Alabyev, B. & Manser, T. Initial Clonal Expansion of Germinal Center B Cells Takes Place at the Perimeter of Follicles. *Immunity* **30**, 599–609 (2009).

100.	Kambayashi, T. & Laufer, T. M. Atypical MHC class II-expressing antigen-presenting cells: can anything replace a dendritic cell? *Nat. Rev. Immunol.* **14**, 719–730 (2014).

101.	Rose, S., Misharin, A. & Perlman, H. A novel Ly6C/Ly6G-based strategy to analyze the mouse splenic myeloid compartment. *Cytometry A* **81A**, 343–350 (2012).

102.	Gentek, R., Molawi, K. & Sieweke, M. H. Tissue macrophage identity and self-renewal. *Immunol. Rev.* **262**, 56–73 (2014).

103.	Davies, L. C., Jenkins, S. J., Allen, J. E. & Taylor, P. R. Tissue-resident macrophages. *Nat. Immunol.* **14**, 986 (2013).

104.	Köhler, C. Allograft inflammatory factor-1/Ionized calcium-binding adapter molecule 1 is specifically expressed by most subpopulations of macrophages and spermatids in testis. *Cell Tissue Res.* **330**, 291–302 (2007).

105.	Chistiakov, D. A., Killingsworth, M. C., Myasoedova, V. A., Orekhov, A. N. & Bobryshev, Y. V. CD68/macrosialin: not just a histochemical marker. *Lab. Invest.* **97**, 4–13 (2017).

106.	Mainardi, S. *et al.* Identification of cancer initiating cells in K-Ras driven lung adenocarcinoma. *Proc. Natl. Acad. Sci.* **111**, 255–260 (2014).

107.	Mertens, C. *et al.* Intracellular Iron Chelation Modulates the Macrophage Iron Phenotype with Consequences on Tumor Progression. *PLOS ONE* **11**, e0166164 (2016).

108.   Kim, H. A. *et al.* Brain immune cell composition and functional outcome after cerebral ischemia: comparison of two mouse strains. *Front. Cell. Neurosci.* **8**, 365 (2014).

109.   Pereira-Lopes, S. *et al.* NBS1 is required for macrophage homeostasis and functional activity in mice. *Blood* **126**, 2502–2510 (2015).

110.   Rackov, G. *et al.* p21 mediates macrophage reprogramming through regulation of p50-p50 NF-κB and IFN-β. *J. Clin. Invest.* **126**, 3089–3103 (2016).

111.   Franken, L. *et al.* Splenic red pulp macrophages are intrinsically superparamagnetic and contaminate magnetic cell isolates. *Sci. Rep.* **5**, 12940 (2015).

ACKNOWLEDGMENTS

I would like to thank to my supervisor, Professor Pier Giuseppe Pelicci, for giving me the opportunity to work in his laboratory on this incredible project, for the scientific discussions and for his guidance through my PhD years.

I would like to give special thanks to my added supervisor, Dr. Maria Vittoria Verga Falzacappa (MaVi) with whom I have worked closely for four years on this project: Thank you for being the best supervisor I could ever asked for, for teaching me how to grow as a scientist and a person, and how to look at the things from different angles, for your moral support throughout these years and for being a friend.

I would also like to thank to my internal and external advisors, Dr. Bruno Amati and Professor Andreas Kulozik, for their constructive comments and suggestions that contributed to my thesis work.

To all the friends I met during the PhD program, especially to Giorgia Ceccotti: Thank you for the great times in the lab and outside of it.

To my sister Nina, my parents and Filip, for always being there for me. Your love and support mean the world to me.